Received: 7 September 2022 | Revised: 2 December 2022 | Accepted: 6 January 2023

DOI: 10.1111/bph.16035

RESEARCH ARTICLE

Differential regulation of $Ca_v3.2$ and $Ca_v2.2$ calcium channels by CB_1 receptors and cannabidiol

Erika K. Harding[1,2,3] | Ivana A. Souza[2,3] | Maria A. Gandini[2,3] | Vinícius M. Gadotti[2,3,4] | Md Yousof Ali[2,3,4] | Sun Huang[2,3] | Flavia T. T. Antunes[2,3] | Tuan Trang[1,2,3] | Gerald W. Zamponi[2,3]

[1]Department of Comparative Biology and Experimental Medicine, University of Calgary, Calgary, AB, Canada

[2]Department of Clinical Neurosciences, and Physiology & Pharmacology, University of Calgary, Calgary, AB, Canada

[3]Hotchkiss Brain Institute, University of Calgary, Calgary, AB, Canada

[4]Zymedyne Therapeutics, Calgary, AB, Canada

Correspondence
Gerald W. Zamponi, Department of Clinical Neurosciences,iversity of Calgary, Calgary, AB, Canada.
Email: zamponi@ucalgary.ca

Funding information
Alberta Innovates; Canadian Institutes of Health Research; Mitacs

Background and Purpose: Cannabinoids are a promising therapeutic avenue for chronic pain. However, clinical trials often fail to report analgesic efficacy of cannabinoids. Inhibition of voltage gate calcium (Ca_v) channels is one mechanism through which cannabinoids may produce analgesia. We hypothesized that cannabinoids and cannabinoid receptor agonists target different types of Ca_v channels through distinct mechanisms.

Experimental Approach: Electrophysiological recordings from tsA-201 cells expressing either $Ca_v3.2$ or $Ca_v2.2$ were used to assess inhibition by HU-210 or cannabidiol (CBD) in the absence and presence of the CB_1 receptor. Homology modelling assessed potential interaction sites for CBD in both $Ca_v2.2$ and $Ca_v3.2$. Analgesic effects of CBD were assessed in mouse models of inflammatory and neuropathic pain.

Key Results: HU-210 (1 μM) inhibited $Ca_v2.2$ function in the presence of CB_1 receptor but had no effect on $Ca_v3.2$ regardless of co-expression of CB_1 receptor. By contrast, CBD (3 μM) produced no inhibition of $Ca_v2.2$ and instead inhibited $Ca_v3.2$ independently of CB_1 receptors. Homology modelling supported these findings, indicating that CBD binds to and occludes the pore of $Ca_v3.2$, but not $Ca_v2.2$. Intrathecal CBD alleviated thermal and mechanical hypersensitivity in both male and female mice, and this effect was absent in $Ca_v3.2$ null mice.

Conclusion and Implications: Our findings reveal differential modulation of $Ca_v2.2$ and $Ca_v3.2$ channels by CB_1 receptors and CBD. This advances our understanding of how different cannabinoids produce analgesia through action at different voltage-gated calcium channels and could influence the development of novel cannabinoid-based therapeutics for treatment of chronic pain.

KEYWORDS
cannabidiol, cannabinoid receptor, CB_1 receptors, $Ca_v2.2$, $Ca_v3.2$, T-type calcium channel, voltage-gated calcium channel

Abbreviations: CFA, Complete Freund's Adjuvant; DRG, dorsal root ganglion; tsA-201, transformed human kidney cell line expressing an SV40 temperature-sensitive T antigen; VGCC, voltage-gated calcium channel.

1 | INTRODUCTION

The potential utility of cannabinoids in treating chronic pain remains unclear, with many clinical trials reporting limited efficacy (Fisher et al., 2021; Vela et al., 2022; but see Whiting et al., 2015). Despite this, many patients report that use of cannabinoids such as **Δ^9-tetrahydrocannabinol (THC)** or **cannabidiol (CBD)** reduces their pain (Baron et al., 2018; Boehnke et al., 2016; Ware et al., 2005). Additional studies are therefore needed to understand to what extent and the mechanisms underlying how cannabinoids produce analgesia.

Voltage-gated calcium channels (VGCCs; Ca_vs) are a promising target for the treatment of chronic pain due to their role in regulating neuronal excitability and facilitating synaptic vesicle release at primary afferent synapses (Harding & Zamponi, 2022). First-order neurons transmit nociceptive information from peripheral tissue into the dorsal horn of the spinal cord, where neurotransmission onto dorsal horn neurons is predominantly facilitated by two presynaptic VGCCs: **$Ca_v2.2$ (N-type)** and to a lesser extent **$Ca_v3.2$ (T-type)** channels (Zamponi, 2016).

Cannabinoids like THC inhibit vesicular release through activation of the presynaptic **CB_1 receptor** and subsequent G protein-mediated inhibition of presynaptic calcium channels and activation of G protein-coupled **inwardly rectifying (GIRK; K_{IR}) potassium channels**. The regulation of $Ca_v2.2$ channels by G protein-coupled receptors is well documented and typically involves the induction of a reluctant gating state by binding of the G protein βγ dimer to the pore forming α1 subunit of the channel (di Marzo et al., 2004; Mackie & Hille, 1992; Tedford & Zamponi, 2006; Twitchell et al., 1997). However, less is known as to whether and how cannabinoid receptors regulate $Ca_v3.2$ channels.

Conversely, CBD appears to exert its pharmacological action in a non-canonical manner. Many studies have demonstrated that the affinity of CBD as an agonist for CB_1 receptors is very low (Mlost et al., 2020; Pertwee, 2008) and that CBD may instead act as a non-competitive allosteric modulator of CB_1 receptors at low micromolar concentrations (Laprairie et al., 2015). Other studies have indicated that CBD acts as a modulator of fatty acid hydrolysis, or an agonist at **TRPV1 receptors**, **5-HT_{1A}** receptors and **K_v7 channels** (Bisogno et al., 2001; de Gregorio et al., 2019; Zhang et al., 2022). Additionally, *in vitro* studies suggest that CBD can act as an antagonist of low voltage-activated VGCCs including $Ca_v3.2$ (Ross et al., 2008).

Despite the mechanism of action being unclear, preclinical studies consistently demonstrate that CBD produces analgesia, notably in rodent models of arthritic and neuropathic pain (de Gregorio et al., 2019; Finn et al., 2021; Philpott et al., 2017; Ward et al., 2014). Moreover, administration of CBD appears to boost the efficacy of administered opioids in the treatment of chronic pain (Boehnke et al., 2016; Jesus et al., 2022).

Here, we show that CB_1 receptors potently modulate N-type, but not T-type calcium channels, whereas CBD inhibits the activity of the latter but not the former calcium channel subtype. Furthermore, we show that at the spinal level, CBD-mediated analgesia is dependent on $Ca_v3.2$.

What is already known

- Cannabinoids like THC inhibit high voltage-activated calcium channels like $Ca_v2.2$ through CB_1 receptor activation.
- In preclinical studies, CBD produces analgesia despite having minimal activation of the CB_1 receptor.

What does this study add

- Cannabinoid receptor activation does not produce inhibition of the low voltage-activated calcium channel $Ca_v3.2$.
- CBD directly inhibits $Ca_v3.2$, and analgesia obtained through spinally administered CBD is $Ca_v3.2$ dependent.

What is the clinical significance

- Understanding the mechanisms by which cannabinoids produce analgesia will better inform development of novel analgesics.

2 | METHODS

2.1 | Cell culture and transfections of tsA-201 cells

Human embryonic kidney tsA-201 cells (RRID:CVCL_2737) were grown in Dulbecco's modified Eagle's medium (DMEM) containing 10% foetal bovine serum and 1% penicillin/streptomycin. Cells were maintained at 37°C under a humidified atmosphere containing 5% CO_2. Cells were suspended by 0.25% trypsin with ethylenediaminetetraacetic acid (EDTA) and plated on glass coverslips placed within 10 cm culture dishes 6 h before transfection. Using the calcium phosphate method, cells were transiently transfected with 0.5 μg of GFP cDNA (Addgene # 6085-1) and 3 μg of each plasmid encoding the following cDNAs: Human $Ca_v3.2$ α1 subunit (Dr. Terrance Snutch, University of British Columbia, Vancouver, Canada) or rat $Ca_v2.2$ α1 subunit (with the auxiliary rat β1b and rat α2δ1 subunits) (Dr. Terrance Snutch, University of British Columbia, Vancouver, Canada) with or without the human CB_1 receptor (Dr. Ken Mackie, Indiana University, Bloomington, USA). After 20 h, media was changed and cells were placed into a 30°C incubator. Cells were used for experiments 72 h post-transfection. For co-immunoprecipitation experiments, no GFP plasmid was included during transfection, cells were maintained in 37°C throughout the entire 72-h incubation, and a rat $Ca_v2.2$-GFP tagged α1 subunit was used for blotting against GFP.

2.2 | Dorsal root ganglion (DRG) neuron isolation

DRGs from the spinal lumbar section level 4–6 of 5-week-old C57Bl/6 male mice were harvested and cut into small pieces and incubated with 4 $mg{\cdot}mL^{-1}$ collagenase (Gibco) and 40 $\mu L{\cdot}mL^{-1}$ papain (Worthington) in culture medium (Dulbecco's modified Eagle's medium, Gibco) supplemented with 10% heat-inactivated fetal bovine serum (Gibco) and 1% penicillin/streptomycin (Gibco) at 37°C for 30 min, followed by 1 $\mu g{\cdot}mL^{-1}$ DNase (Sigma) for another 10 min. After that, digested DRG tissue was washed three times with culture medium and mechanically dissociated into single cells. DRG neurons were plated on glass coverslips pretreated with Poly-D-Lysine (Sigma) and Laminin (Sigma) and maintained at 37°C in a 5% CO_2 incubator. Electrophysiological recordings were performed within 24 h after plating.

2.3 | Electrophysiology

For tsA-201 cells, whole-cell voltage-clamp recordings were performed at room temperature (20–22°C) 72 h after transfection as previously described (Gandini et al., 2019). Currents were recorded in pCLAMP9.2 using an Axopatch 200B amplifier and digitized via a Digidata 1322A (Molecular Devices, San Jose, USA). The external solution consisted of (in mM): 10 $BaCl_2$, 125 CsCl, 1 $MgCl_2$, 10 HEPES and 10 glucose (pH 7.4 adjusted with CsOH). Patch pipettes (Sutter Instrument Co., Novato, CA, 2–4 MΩ) were filled with an internal solution containing (in mM): 130 CsCl, 2.5 $MgCl_2$, 5 EGTA, 10 HEPES, 3 Na-ATP, and 0.5 Mg-GTP (pH 7.4 adjusted with CsOH). Junction potential was calculated as less than 0.7 mV (Junction Potential Calculator, Clampex 11.2, Molecular Devices, San Jose, USA) and was thus left uncorrected.

Current–voltage relationships of $Ca_v3.2$ were determined by applying 200 ms pulses between −60 mV and +20 mV in 5 mV increments from a holding potential of −110 mV. Current was converted into current density by dividing the peak current at each voltage by the cell capacitance. Obtained I-V curves were fitted using the following Boltzmann equation: $(I = ((V_{mem} - V_{rev}) \times G_{max})/(1 + \exp(V_{mem} - V_a)/d_x))$, where I is the peak current, V_{mem} is the membrane potential, V_{rev} is the reversal potential, G_{max} is the maximum conductance, V_a is the half voltage for activation and d_x is the slope factor.

Steady-state inactivation curves of $Ca_v3.2$ were obtained by applying 800 ms conditioning prepulses from −110 to −20 mV in 10 mV increments followed by a 100 ms test pulse to − 20 mV. Curves were fitted with the equation: $I/I_{max} = 1/(1 + \exp(V_h - V_{mem})/d_x)$, where V_h is the half inactivation potential.

Perfusion time courses were obtained by applying 200 ms pulses to −20 mV from a holding potential of −110 mV every 20 s for up to 15 min for $Ca_v3.2$ and pulses to +20 mV from a holding potential of −100 mV for $Ca_v2.2$. Percent inhibition was calculated between the last sweep before drug perfusion began and 400 s into the recording.

To ascertain the dose dependence of CBD action on $Ca_v3.2$, recordings were performed as described previously (Gadotti et al., 2021). Briefly, the external solution contained (in mM): 40 TEACl, 65 CsCl, 20 $BaCl_2$, 1 $MgCl_2$, 10 HEPES and 10 glucose, pH adjusted to 7.4. The internal solution contained (in mM): 140 CsCl, 2.5 $CaCl_2$, 1 $MgCl_2$, 5 EGTA, 10 HEPES, 2 Na-ATP, and 0.3 Na-GTP, pH adjusted to 7.3. Patch clamp recordings were performed by an EPC 10 amplifier linked to a personal computer equipped with Pulse (V8.65) software (HEKA Elektronik, Bellmore, USA). Junction potential was calculated as 2.8 mV (Junction Potential Calculator, Clampex 11.2, Molecular Devices, San Jose, USA) and was thus left uncorrected. Inward current was elicited by 300 ms depolarization from a holding potential of −110 mV to a test potential of −20 mV with an interpulse interval of 20 s. Each cell was subjected to only one concentration of CBD and % inhibition was calculated over a 15 sweep period, comparing the first sweep to an average of the last three sweeps. The number of cells recorded for each concentration of CBD was less than 5 due to the exploratory nature of this experiment and therefore represents preliminary data.

All cells were recorded with series resistance compensation. Recordings were performed with randomization, recording from equal numbers of cells each day for each condition. In order to ensure adequate randomization between groups (especially with respect to peak current and cell capacitance), the experimenter could not be blinded to condition during experiments. Data analysis was performed blinded to condition where possible. For perfusion experiments, cells were excluded from analysis if access resistance changed by more than 20% during recordings, or if cells were lost before perfusion could be completed. Cells were excluded from I-V analysis if they were unstable or had peak current less than 15 $pA{\cdot}pF^{-1}$ or greater than 150 $pA{\cdot}pF^{-1}$. Cells that were excluded were not replaced, thus resulting in nonequal group sizes. Group sizes were determined based on previous publications (Gadotti et al., 2021; Gandini et al., 2019).

For recordings of DRG neurons, recordings were performed as described previously (Gadotti et al., 2021). Briefly, the external solution contained the following (in mM): 40 TEACl, 65 CsCl, 20 BaCl2, 1 MgCl2, 10 HEPES and 10 glucose, pH adjusted to 7.4. The internal solution contained the following (in mM): 140 CsCl, 2.5 CaCl2, 1 MgCl2, 5 EGTA, 10 HEPES, 2 Na-ATP and 0.3 Na-GTP, pH adjusted to 7.3. Patch clamp recordings were performed by an EPC 10 amplifier linked to a personal computer equipped with Pulse (V8.65) software (HEKA Elektronik, Bellmore, USA). To isolate low voltage-activated voltage-gated calcium channel current, the stimulation protocol was altered slightly. For these experiments, DRG neurons were maintained at −90 mV, with a 300 ms depolarization to a test potential of −30 mV. All other conditions remained the same between these experiments.

2.4 | Co-immunoprecipitation assays and western blots

All immunoblotting experiments comply with the recommendations made by the *British Journal of Pharmacology* (Alexander et al., 2018). In

experiments with tsA-201 cells, cells were washed once with ice-cold Hepes-based saline solution and then lysed in a modified RIPA buffer (50-mM Tris, 150-mM NaCl, 0.25% Triton X-100, pH 7.5) containing 1× Complete protease inhibitor cocktail. Lysates were centrifuged at 13,000 rpm for 20 min at 4°C to remove cell debris and protein concentration was quantified from supernatants using the BioRad protein assay dye. One milligram of lysates was incubated in RIPA buffer with 2 µg of either anti-CB_1 receptor (Abcam, #23703) or anti-$Ca_v3.2$ (Novus Biologicals, #NBP1-22444) antibodies overnight at 4°C with rotation, followed by immunoprecipitation for 1.5 h using protein A or G Sepharose beads, respectively. Immunoprecipitates were washed 3× in RIPA buffer and eluted with 2× Laemmli sample buffer. Proteins were resolved using SDS-PAGE, transferred to polyvinylidene fluoride membranes (Immun-Blot polyvinylidene fluoride membranes [PVDF], Bio-Rad, #1620177) and immunoblotted with one of the following primary antibodies: anti-CB_1 receptor (Abcam, 23703, RRID:AB_447623, 1:250), anti-Ca_v 3.2 (Novus Biologicals, #NBP1-22444, RRID:AB_1659986, 1:250) or anti-GFP (Abcam, #ab1218, RRID:AB_298911, 1:500) overnight at 4°C. Membranes were then incubated with horseradish peroxidase-linked anti-mouse or anti-rabbit antibodies and developed using SuperSignal West Dura substrate (Thermo Scientific) and a C-DiGit blot scanner (LI-COR).

In experiments with tissue, whole brains (mBr) from C57Bl/6 and $Ca_v3.2$ null animals were removed and homogenized in ice cold 0.32 M glucose solution. Proteins were obtained using a buffer containing 50-mM Tris (pH 7.5), 150 mM NaCl, 1% Igepal, 10% (w/v) glycerol and 1× Complete protease inhibitor cocktail. Lysates were centrifuged at 13,000 rpm for 10 min at 4°C, rehomogenized, centrifuged again, and the supernatant collected. Protein concentration was quantified using the BCA assay. Two milligrams of lysates were incubated with 3 µg of anti-CB_1 receptor (Cayman, #211-032-171) or anti-Nurr1 (IgG0 control, Santa Cruz, #N-20, RRID:AB_2153906) antibodies overnight at 4°C with rotation, followed by immunoprecipitation for 2 h using a mix of protein A and G Sepharose beads. Immunoprecipitates were washed three times in lysis buffer and two times in PBS and eluted with 2× Laemmli (containing 50 mM DTT and 0.5 M β-mercaptoethanol) sample buffer. Proteins were resolved using SDS-PAGE, transferred to nitrocellulose membranes (BioRad) and immunoblotted using anti-$Ca_v3.2$ (Santa Cruz, #H-300). Membranes were then incubated with horseradish peroxidase-linked anti-rabbit antibody (Jackson Immunolab, #211-032-171, RRID:AB_2339149) and developed using SuperSignal West Dura substrate (Thermo Scientific) and a C-DiGit blot scanner (LI-COR).

2.5 | Animals

In vivo experiments were carried out following approval of an animal protocol by the Institutional Animal Care and Use Committee at the University of Calgary. Adult (8–12 weeks) male or female C57Bl/6J mice purchased from Jackson Laboratories were used and adult male (8–12 weeks) male $Ca_v3.2$ null mice were produced in house from breeding pairs originally obtained from Jackson Laboratories (strain #013770) (Chen et al., 2003). Mice were kept at a maximum of five per cage (30 × 20 × 15 cm) in controlled temperature of 23 ± 1°C on a 12 h light/dark cycles (lights on at 7:00 a.m.) and with free access to food and water. Experiments were performed between 10 AM and 3 PM, and different cohorts of mice were used for each testing session. *In vitro* experiments were carried out on male C57Bl/6J mice (5 weeks) produced in house from breeding pairs originally purchased from Jackson Laboratories. For these experiments mice were euthanized by an overdose of isoflurane followed by decapitation. Animal studies are reported hereafter in compliance with the ARRIVE guidelines (Percie du Sert et al., 2020) and with the recommendations made by the *British Journal of Pharmacology* (Lilley et al., 2020).

Injections via intrathecal (i.t.) route were performed in fully conscious mice according to routinely performed in our lab (Gadotti et al., 2013, 2015). The dorsal fur of each mouse was shaved 24 h prior to injection. Animals were manually restrained, the spinal column was arched and a 30-gauge needle attached in a PE20 Polyethylene tube to a 25 µL Hamilton microsyringe (Hamilton, Birmingham, UK) was inserted into the subarachnoid space between the L4 and L5 vertebrae. Positioning of the needle tip was confirmed by a characteristic tail-flick response of animal when the needle is correctly positioned. Intrathecal injections of 10 µL were delivered over a period of a minimum of 5 s.

2.6 | Pain models

The formalin test was performed as originally described (Hunskaar et al., 1985) and as previously performed by our lab (Gadotti et al., 2013, 2015). Mice were always allowed to acclimatize in the laboratory for at least 60 min before experiments. They received a volume of 20 µL of a formalin solution (2.5%) prepared in PBS injected intraplantarly (i.pl.) in the ventral surface of the right hindpaw. After formalin injection, mice were immediately kept individually in observation chambers and the time spent licking or biting the injected paw was recorded and considered as nocifensive response. We scored the nociceptive responses of each animal individually from 0 to 5 min (neurogenic phase) and 15 to 30 min (inflammatory phase). CBD (2.5% DMSO in PBS) or vehicle (2.5% DMSO in PBS) was administrated spinally (i.t.) 20 min prior to receiving formalin and its effect on both nociceptive and inflammatory phases of the formalin test were analysed.

Complete Freund's Adjuvant (CFA) was used to induce thermal hyperalgesia produced by peripheral inflammation. Twenty microliters (20 µL) of CFA) were injected subcutaneously in the plantar surface of the right hindpaw (intraplantar) (Ferreira et al., 2001). Sham groups received 20 µL of PBS in the ipsilateral paw. Two days after CFA injection, mice were treated with either CBD or vehicle delivered spinally (i.t.) and their thermal withdrawal threshold was tested.

Chronic neuropathic pain was induced by a partial sciatic nerve ligation injury (PSNL) where a single tight ligature around a third to a half of the diameter of the sciatic nerve was performed. Mice were anaesthetized with isoflurane (5% induction, 2.5% maintenance) and monitored for respiration and spontaneous breathing throughout the

surgery. Fur around the upper right leg was shaved, and the area was then disinfected with 70% ethanol and skin was cut with a surgical blade. Leg muscle was separated by blunt dissection to expose the sciatic nerve. The right sciatic nerve was then exposed proximal to the sciatic nerve trifurcation. Sham-operated mice had nerves exposed but no ligatures placed (Malmberg & Basbaum, 1998). Skin was re-sutured with 4.0 vicryl sutures (3–4). Due to the short length of surgeries no heat support was provided during surgery, but a heating pad was placed under half of the cage to aid recovery from anesthesia. Mice were monitored for up to one hour post-surgery to ensure successful recovery from anesthesia. Experiments were always performed using two different cohorts of mice. Mice received CBD or vehicle intrathecally 3 weeks after nerve injury and were tested for mechanical hyperalgesia. Mice were randomly assigned to sham or partial sciatic nerve ligation surgery cohorts and CBD or vehicle cohorts, with the goal of creating equal group sizes where litter size allowed. Group sizes were determined based on previous publications (Gadotti et al., 2021). The experimenter could not be blinded to condition due to effect size. Mice were monitored once daily for 7 days to ensure sutures were holding and mice recovered well from surgery. All mice healed well and were included in behavioural experiments.

2.7 | Behaviour

Thermal hyperalgesia was analysed by measuring the latency to withdrawal of right hind paws on a focused beam of radiant heat (IR = 30) of a Plantar Test apparatus (UgoBasile, Varese, Italy). Animals were placed individually in a small, enclosed testing arena (20 cm × 18.5 cm × 13 cm, length × width × height) on top of a plastic glass floor and they were allowed to acclimate for a period of at least 90 min before testing. The radiant heat source was positioned beneath the animal, so that the heat was directly under the plantar surface of the ipsilateral hind paw. Each mouse was tested three times for each timepoint: Prior to the treatments (Time 0) and 30, 60, 120 and 180 min after intrathecal treatment with CBD or vehicle. The device has a cut-off time of 30 s to avoid tissue damage.

Mechanical hyperalgesia was measured using a digital plantar aesthesiometer (DPA, Ugo Basile). Animals were placed individually in a small, enclosed testing arena on top of a grid platform (digital plantar aesthesiometer). The device was placed beneath the testing floors so the filament could be moved and positioned accurately under the plantar surface of the ipsilateral hind paw of each animal. Each paw was tested three times per session (García-Caballero et al., 2014). Animals without thermal or mechanical pain phenotypes in response to CFA, formalin, or PSN surgery were not used for experimentation. No other animals were excluded from analysis.

2.8 | Materials

CBD was obtained from Cayman Chemicals (Ann Arbor, Michigan, USA) (#90080, ≥98% purity) and dissolved in 100% DMSO to form stock aliquots at 3 mM. HU-210 was obtained from Toronto Research Chemicals (Toronto, Canada) (#H673500) and dissolved in 100% DMSO to form stock aliquots at 10 mM. Final concentrations in external solution ensured less than 0.1% DMSO, which served as perfusion control. Complete Freund's Adjuvant (CFA) was obtained from Sigma Aldrich, (#5881). Formalin was obtained from Merck Millipore (Burlington, Massachusetts, USA) (#R04586). Unless otherwise stated, all other chemicals were obtained from Millipore-Sigma. Details of other materials and suppliers were provided in the specific sections.

2.9 | Molecular docking

The starting model of $Ca_v3.2$ was made in ColabFold (Mirdita et al., 2022) based on the structure of the human $Ca_v3.1$ α 1G subunit (Zhao et al., 2019). The structures of the human N-type voltage gated calcium channel $Ca_v2.2$-α2δ1-β1 complex were obtained from the RCSB Protein Data Bank (PDB ID: 7VFW) (Dong et al., 2021). The protein was prepared using Accelrys Discovery Studio 19.1 (Accelrys, San Diego, CA, USA). The reported binding area between co-ligand and the protein was considered the most affirmative region for the ligand binding docking simulation. Next, the reported compound blocker 1 was removed and the protein was regarded as ligand free (Dong et al., 2021). Water molecules were also removed from the protein structure for docking simulation. Polar hydrogen atoms were added into the protein using an automated docking tool, AutoDock 4.2.6 (Goodsell et al., 1996; Jones et al., 1997). The docking studies for the CBD and co-crystalline ligand were performed without modifying the default parameters. The 2D structure of CBD was drawn with MarvinSketch (ChemAxon, Budapest, Hungary) and converted into 3D pdb format using Chem3D Pro software (v12.0, Cambridge Soft Inc., Cambridge, MA, USA). Energy minimization of each ligand were carried out using molecular mechanics 2 (MM2) force field. The docking analysis was conducted using Autodock Vina (Trott & Olson, 2009). A grid box size of 60 × 60 × 60 points with spacing of 1.0 Å between the gird points was executed to cover almost the entire favourable protein binding site. The X, Y, Z centres were for $Ca_v2.2$ (167.047186, 169.790978 and 154.958226) and $Ca_v3.2$ (−3.606705, 1.964202 and −2.723603). The docking protocol for rigid and flexible ligand docking comprised 20 independent genetic algorithms. In docking studies, the selected ligand CBD was examined for qualified binding poses. The binding aspect of $Ca_v2.2$ and $Ca_v3.2$ residues and their corresponding binding affinity score are regarded as the best molecular interaction. All structure figures were prepared in Discovery Studio Visualizer and PyMol. All docking simulations were performed using Intel® Core™ i7-4510 CPU @ 32.00 GHz with Windows 10 and a 64-bit operating system with the molecular docking simulation environment.

2.10 | Data analysis

The data and statistical analyses comply with the recommendations of the *British Journal of Pharmacology* on experimental design and

analysis in pharmacology (Curtis et al., 2022). Data were normalized in the following experiments: Steady-state inactivation curves, perfusion time courses and % inhibition. Steady-state inactivation curves were normalized within each cell to the peak current obtained with a pre-pulse matching resting membrane potential. This is necessary as peak current can vary widely between cells and could obscure the actual half-inactivation voltage. Time courses and % inhibition were normalized within each cell to the current at time 0. This is necessary as peak current can vary widely between cells and could artificially skew drug effects to that observed in cells with larger current. By normalizing to initial current, we give each cell equal weight to properly observe average drug effects on current. These normalized data were expressed and plotted as % of initial current or peak current to reflect this within cell normalization. Each stated n value represents the number of independent values and statistical analysis was performed on these independent values.

All data were analysed using Prism 9.4.1 (Graphpad Software, San Diego, USA). All averaged data are plotted as mean ± SEM. Statistical analysis was performed only on groups with an n of at least 5 and as follows. First, each data set was analysed for outliers (ROUT, Q = 1%) and tested for normality (Shapiro–Wilk test, $P > 0.05$ = passed). No data met the threshold to be excluded as an outlier and therefore all data were included for analysis. Data comparing a group before and after drug administration were analysed by paired *t* test if data were normal, or Wilcoxon signed rank test if they failed the Shapiro–Wilk test. Comparisons between two sets of data were performed by Student's *t* test if data were normal, or Mann–Whitney test if they failed the Shapiro–Wilk test. Comparisons between multiple sets of data with one variable were performed by one-way ANOVA if data were normal, or by Kruskall–Wallis test if they failed the Shapiro–Wilk test. Comparisons between multiple sets of data with two variables were performed by two-way ANOVA with no matching. All post hoc comparisons were performed by Holm–Sidak comparison, only if tested ANOVA variables achieved statistical significance ($P < 0.05$). Statistical significance was defined as follows: $^*P < 0.05$.

2.11 | Nomenclature of targets and ligands

Key protein targets and ligands in this article are hyperlinked to corresponding entries in the IUPHAR/BPS Guide to PHARMACOLOGY http://www.guidetopharmacology.org and are permanently archived in the Concise Guide to PHARMACOLOGY 2021/22 (Alexander, Christopoulos, et al., 2021; Alexander, Mathie, et al., 2021).

3 | RESULTS

3.1 | Expression of the CB_1 receptor with $Ca_v3.2$ does not change baseline channel properties

We began by transfecting either human $Ca_v3.2$ channel alone or with human CB_1 receptor in a transformed human kidney cell line expressing an SV40 temperature-sensitive T antigen (tsA-201 cells), followed by investigation of channel function through whole cell patch clamp recordings (Figure 1a). The current–voltage relation showed no shift in the voltage dependence of activation or peak voltage and no difference in peak current density between cells transfected with $Ca_v3.2$ only or both $Ca_v3.2$ and CB_1 receptor (Figure 1b,c). Furthermore, steady-state inactivation curves were recorded with prepulses between −110 and −20 mV demonstrating no difference in the voltage-dependence of inactivation between conditions (Figure 1d,e). Therefore, expression of CB_1 receptor does not alter baseline properties or expression of $Ca_v3.2$.

3.2 | The synthetic cannabinoid HU-210 inhibits $Ca_v2.2$, but not $Ca_v3.2$ through a CB_1 receptor dependent mechanism

Since CB_1 receptor activation inhibits $Ca_v2.2$ (Mackie & Hille, 1992; Twitchell et al., 1997), we next determined whether application of the synthetic CB_1 receptor agonist HU-210 may also modulate the activity of $Ca_v3.2$. In a positive control experiment recording from cells transfected with both $Ca_v2.2$ and CB_1 receptor, perfusion of the synthetic cannabinoid HU-210 (1 μM) produced a significant inhibition of current over time (Figure 2a). Conversely, perfusion of HU-210 produced no inhibition of inward current through $Ca_v3.2$ (Figure 2b). Maximum inhibition of $Ca_v2.2$ appeared to occur approximately 300 s after HU-210 perfusion. No inhibition was observed during DMSO control perfusion or when HU-210 was perfused in cells transfected with only $Ca_v2.2$ (Figure 2c). By contrast, in cells transfected with $Ca_v3.2$ and CB_1 receptor, no reduction in current was observed in DMSO controls or HU-210. Furthermore, no inhibition of $Ca_v3.2$ was observed with perfusion of the receptor agonist (Figure 2d,g). Quantification of the effects on $Ca_v2.2$ revealed a significant 30.2 ± 4.8% inhibition of inward current through $Ca_v2.2$ during perfusion of HU-210 (Figure 2e). Consistent with voltage-dependent Gβγ modulation by Gi/o-coupled receptors like CB_1 receptor, a brief depolarizing pulse relieved inward current from inhibition (Figure 2f). Together, these results are consistent with $Ca_v2.2$, but not $Ca_v3.2$, being inhibited by activation of CB_1 receptors and subsequent G protein interaction and modulation of channel function.

Many G protein-coupled receptors form physical signalling complexes with Ca_v2 calcium channels (Altier & Zamponi, 2008; Beedle & Zamponi, 2004; Turner et al., 2011). To determine if this is also true for CB_1 receptors, we performed co-immunoprecipitation assays of $Ca_v2.2$ and CB_1 receptors, using a variant of $Ca_v2.2$ fused to GFP. tsA-201 cells were transfected with both $Ca_v2.2$-GFP and the CB_1 receptor, and the CB_1 receptor was immunoprecipitated from cell lysate. Blotting against GFP revealed a band in the 250 kDa range, indicative of a protein complex formed by $Ca_v2.2$ and the CB_1 receptor (Figure 3a). Surprisingly, we also found co-immunoprecipitation of $Ca_v3.2$ and the CB_1 receptor, suggesting that they can also form a protein complex (Figure 3b). To confirm this result in native tissue, we

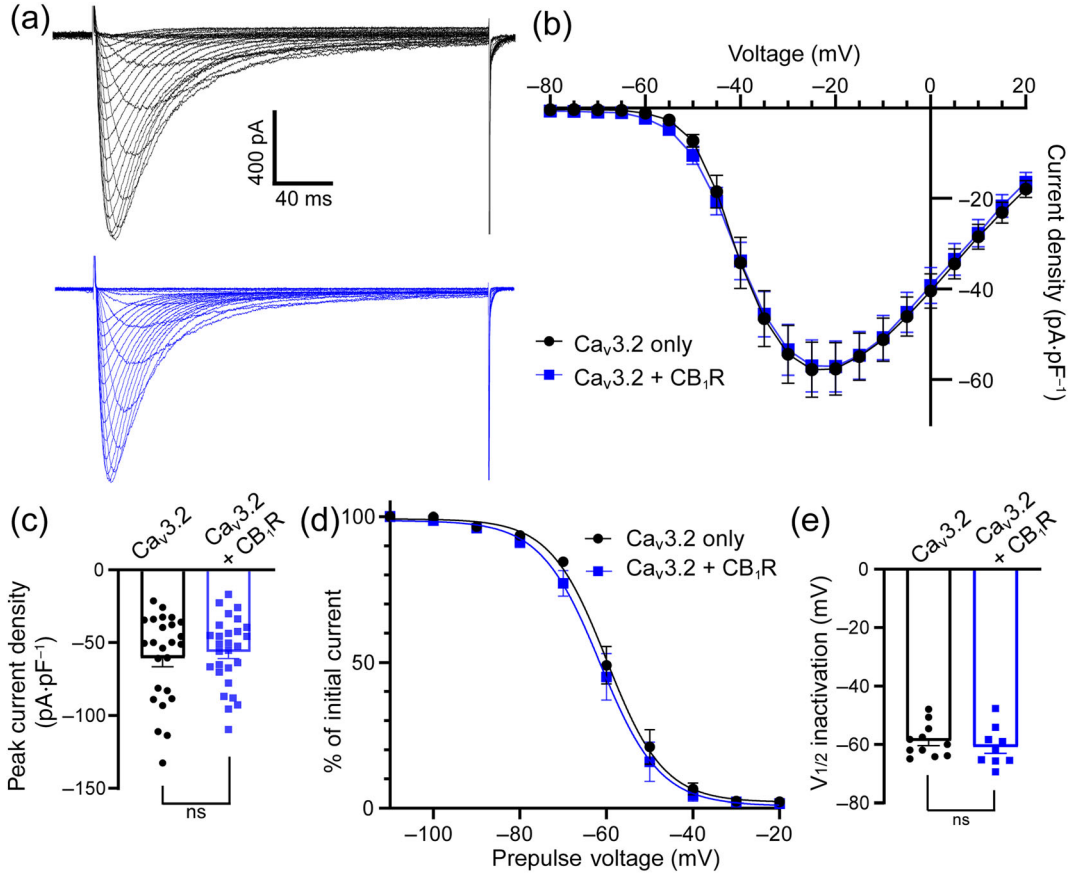

FIGURE 1 Expression of CB_1 receptors (CB_1R) with $Ca_v3.2$ does not change baseline channel properties. (a) Sample whole cell current traces for $Ca_v3.2$ (black) versus CB_1 receptor and $Ca_v3.2$ (blue) expressing cells. Cells were held at −110 mV, with depolarizing pulses from −80 to +20 mV increasing by 5 mV steps with each sweep. (b) Average current–voltage (I-V) relation from cells expressing either $Ca_v3.2$ (black, n = 25 cells) or both $Ca_v3.2$ and CB_1 receptor (blue, n = 30 cells). No difference was observed between the two groups (two-way RM ANOVA, voltage $P < 0.05$, channel expression $P > 0.05$). (c) Comparison of peak current density (Mann–Whitney test, $P > 0.05$, n = 25 cells for $Ca_v3.2$, n = 28 cells for CB_1 receptor and $Ca_v3.2$). (d) Average steady-state inactivation from cells expressing either $Ca_v3.2$ (black, n = 11 cells) or both CB_1 receptor and $Ca_v3.2$ (blue, n = 9 cells) revealing no differences between groups (two-way RM ANOVA, voltage $P < 0.05$, channel expression $P > 0.05$. (e) Comparison of half inactivation voltage (Student's unpaired *t* test, $P > 0.05$, n = 9 cells for $Ca_v3.2$, n = 11 cells for CB_1 receptor and $Ca_v3.2$).

next isolated brain tissue from wild-type and $Ca_v3.2$ null mice. Immunoprecipitation of CB_1 receptors was performed, followed by blotting against $Ca_v3.2$. In tissue from wild-type mice, we found a band in the 250-kDa range, whereas in tissue from $Ca_v3.2$ null mice, no such band was observed (Figure 3c). These data indicate that there are CB_1 receptor-$Ca_v3.2$ complexes in the mouse brain.

Since we found no evidence for CB_1 receptors altering the baseline properties of $Ca_v3.2$, or evidence that activation of CB_1 receptors produces inhibition of $Ca_v3.2$, we hypothesized that perhaps CB_1 receptors and $Ca_v3.2$ may form a complex to regulate reverse trafficking of $Ca_v3.2$ upon CB_1 receptor activation. Indeed, previous studies have found that the CB_1 receptor internalizes after extended exposure to receptor agonists (Hsieh et al., 1999; Jin et al., 1999). However, incubation of cells expressing $Ca_v3.2$ and CB_1 receptors with either a DMSO control or HU-210 for 30 min prior to recording did not affect peak current density (Figure 3d). Together with the observation that $Ca_v3.2$ current densities were unaffected by the presence of the receptor (Figure 1c), these data indicate that although $Ca_v3.2$ and CB_1 receptors form a complex, this does not appear to result in altered forward or reverse trafficking of the channel.

3.3 | The phytocannabinoid CBD triggers inhibition of $Ca_v3.2$, but not $Ca_v2.2$ through a CB_1 receptor-independent mechanism

Next, we sought to define potential interactions between the phytocannabinoid CBD and voltage-gated calcium channels. It has previously been reported that CBD directly inhibits $Ca_v3.2$ (Ross et al., 2008). To confirm these findings, $Ca_v3.2$ was first expressed in tsA-201 cells and various concentrations of CBD were applied to create an exploratory CBD dose–response curve (Figure 4a). Fitting the data revealed an IC50 of 4.06 μM. We therefore chose to further

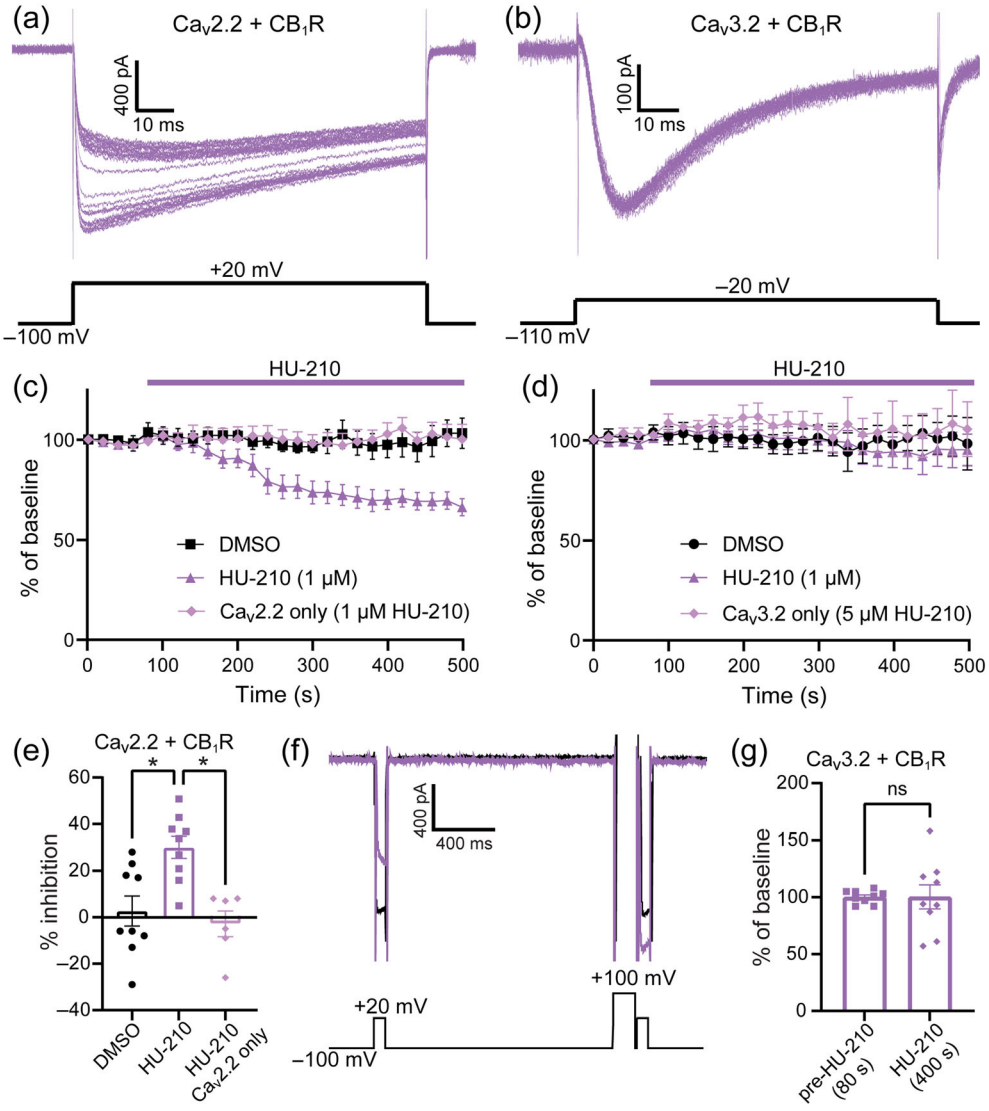

FIGURE 2 The synthetic cannabinoid HU-210 produces inhibition of $Ca_v2.2$, but not $Ca_v3.2$ through a CB_1 receptor (CB_1R)-dependent mechanism. (a,b) Sample traces of calcium channel whole cell current recordings illustrating HU-210 perfusion time courses in tsA-201 cells expressing $Ca_v2.2$ and CB_1 receptor (a) or $Ca_v3.2$ and CB_1 receptor (b), with depolarization pulses to +20 mV (a) or −20 mV (b) every 20 s. (c) Average perfusion time courses for DMSO (black) and HU-210 (purple, 1 μM) plotted as % change in inward current amplitude as compared to baseline in cells expressing $Ca_v2.2$ and CB_1 receptor, or $Ca_v2.2$ only (light purple, 1 μM HU-210). (d) Average perfusion time courses of DMSO (black, n = 9 cells) and HU-210 (purple, 1 μM, n = 10 cells) plotted as % change in inward current amplitude as compared to baseline in cells expressing $Ca_v3.2$ and CB_1 receptor, or $Ca_v3.2$ only (light purple, 5 μM HU-210, n = 6 cells). (e) Quantification of % inhibition of inward current at steady state (t = 400 s), showing significant inhibition only in cells treated with HU-210 and expressing both $Ca_v2.2$ and CB_1 receptor (one-way ANOVA, * $P < 0.05$), followed by post hoc Holm–Sidak comparisons between HU-210 (n = 9 cells) and DMSO (n = 9 cells), ($P < 0.05$) and HU-210 and HU-210 without CB_1 receptor (n = 6 cells), ($P < 0.05$). (f) Sample trace of a cell before (black) and after (purple) perfusion of HU-210, showing voltage-dependent relief from inhibition in the presence of HU-210 consistent with typical Gβγ modulation. (g) Quantification of % change in inward current of cells expressing both $Ca_v3.2$ and CB_1 receptor before and during perfusion of 1 μM HU-210 (Student's paired t test, $P > 0.05$, n = 9 cells).

investigate the potential interactions of CBD when the CB_1 receptor was co-expressed with perfusions of 3 μM CBD to allow for dynamic range for either increased or decreased inhibition. Perfusion of 3 μM CBD produced similar degrees of $Ca_v3.2$ inhibition regardless of expression of CB_1 receptors (Figures 4b and S1). Conversely, in cells expressing $Ca_v2.2$ and CB_1 receptors, no inhibition of $Ca_v2.2$ was observed during perfusion of CBD (Figure 4c). This is consistent with previous reports that micromolar concentrations of CBD are not sufficient to activate CB_1 receptors and also indicates that CBD does not directly inhibit $Ca_v2.2$.

Further characterization of the effect of CBD perfusion on IV-curves revealed that CBD produces a significant inhibition of $Ca_v3.2$ inward current with no shift in activation or peak voltage (Figure 4d,e). Comparison of steady-state inhibition showed that CBD

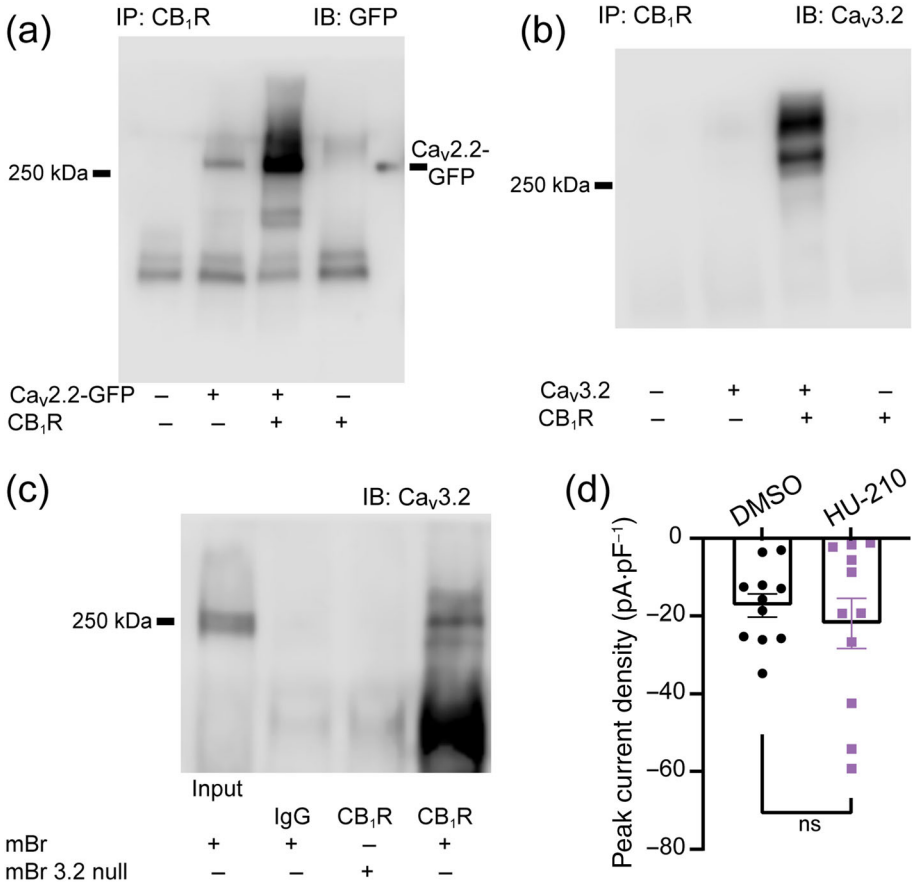

FIGURE 3 Both $Ca_v2.2$ and $Ca_v3.2$ co-immunoprecipitate with CB_1 receptors (CB_1R). (a) Protein from tsA-201 cells expressing GFP-tagged $Ca_v2.2$ and CB_1 receptors was immunoprecipitated using a CB_1 receptor antibody followed by western blot analysis with a GFP antibody. (b) Protein from tsA-201 cells expressing $Ca_v3.2$ and CB_1 receptors was immunoprecipitated using a CB_1 receptor antibody followed by western blot analysis with a $Ca_v3.2$ antibody. (c) Brain tissue from wild-type (mBr) and Cav3.2 null (mBr $Ca_v3.2$) mice were homogenized and immunoprecipitated using a CB_1 receptor antibody followed by western blot analysis with a $Ca_v3.2$ antibody. (d) HU-201 does not internalize $Ca_v3.2$ channels. Cells expressing $Ca_v3.2$ and CB_1 receptors were incubated in either DMSO (black, n = 11 cells) or HU-210 (purple, 0.1 μM, n = 11 cells) for 30 min prior to recording peak current density. Mann–Whitney test, $P > 0.05$.

perfusion produces a significant leftward shift in half inactivation voltage (Figures 4f,g and S1), which was not affected by the presence of CB_1 receptors. Additionally, comparison of percent inhibition at peak current density and the shift in half inactivation voltage between cells expressing $Ca_v3.2$ and those expressing $Ca_v3.2$ and CB_1 receptors revealed no significant difference (Figure 4h,i).

Finally, we performed voltage-clamp recordings of acutely dissociated DRG neurons from wild-type mice. To isolate low voltage-activated calcium currents consistent with T-type calcium channels, cells were maintained at −90 mV, with voltage steps to −30 mV. Perfusion of 3 μM CBD inhibited this inward current by an average of 45.6 ± 4.0% (Figure 4j,k). Together, our data indicate that CBD produces direct inhibition of $Ca_v3.2$ at micromolar concentrations and that this direct inhibition mechanism is not conserved in $Ca_v2.2$. Furthermore, our data support previous studies finding no activation of CB_1 receptors by micromolar concentrations of CBD (Mlost et al., 2020; Pertwee, 2008) and no evidence for CB_1 receptor activation increasing or decreasing the efficacy of inhibition of $Ca_v3.2$ by CBD.

3.4 | Molecular docking explains the differential CBD inhibition of $Ca_v3.2$ and $Ca_v2.2$ channels

To understand why CBD produces direct inhibition of $Ca_v3.2$ but not $Ca_v2.2$, we turned to molecular docking studies to predict possible binding positions of CBD in each channel. We began by creating models of $Ca_v3.2$ and $Ca_v2.2$ α1 subunits for use in Autodock. The structure for $Ca_v2.2$ was derived from the Cryo-electron microscopy structure as previously published (Gao et al., 2021). Cryo-electron microscopy structures exist for $Ca_v3.1$ and $Ca_v3.3$, but not yet for $Ca_v3.2$ (He et al., 2022; Zhao et al., 2019). We thus used Colabfold to create a $Ca_v3.2$ homology model based on the structure of $Ca_v3.1$ (Figure S2).

Molecular docking of CBD with this $Ca_v3.2$ structure revealed that CBD straddles the pore of $Ca_v3.2$ thereby occluding the permeation pathway (Figure 5a). Notably, 3D and 2D modelling of CBD with $Ca_v3.2$ revealed several interactions including a hydrogen bond with Gly365, π-alkyl interactions with Ala992, Ile369, Phe372, Phe241, Val996, Trp990 and Tyr366; an π-sigma interaction with Phe241; and alkyl interactions with Val996 and Ile369 with in the $Ca_v3.2$ channel (Figure S2). The CBD aromatic rings and its alkyl chain are positioned into the central cavity and stabilized by forming π-alkyl interactions with hydrophobic residues. Additionally, the CBD aromatic A-ring occupies the DII-DIII fenestration by hydrophobic residues. Therefore, our results indicate that the $Ca_v3.2$ channel is blocked by CBD with strong hydrophobic interactions by interacting with polar and hydrophobic residues.

Next, molecular docking of CBD with the cryo-EM structure of $Ca_v2.2$ was performed, showing a markedly different positioning that does not appear to block the channel pore (Figure 5b). Unlike with

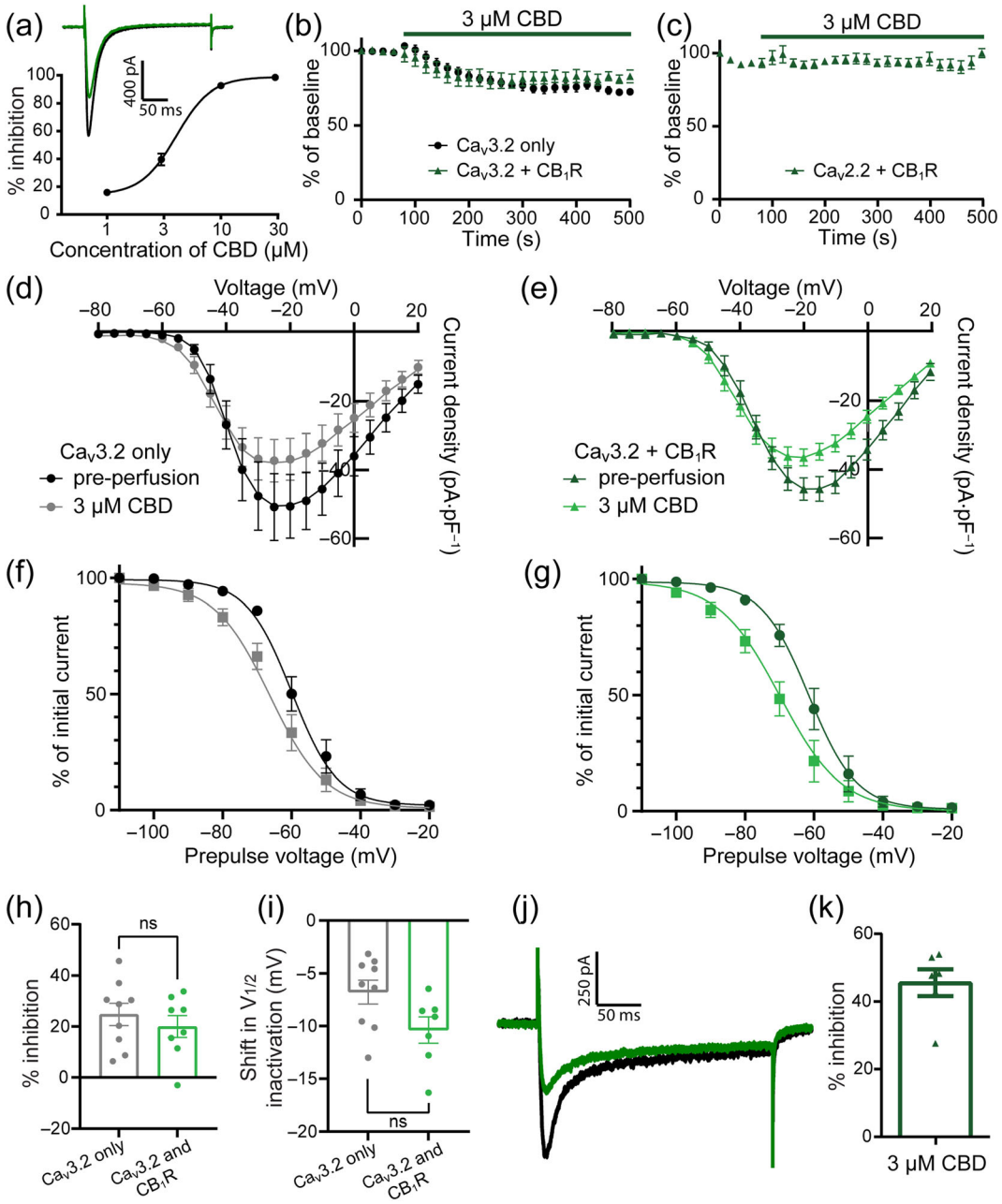

FIGURE 4 Cannabidiol (CBD) inhibits $Ca_v3.2$, but not $Ca_v2.2$ through a CB_1 receptor (CB_1R)-independent mechanism. (a) Dose–response curve of % inhibition of inward current in tsA-201 cells expressing $Ca_v3.2$, n = 4 cells at each concentration. Inset sample trace of inward current before (black) and after (green) perfusion of 3 μM CBD. (b) Time course for perfusion of 3 μM CBD in cells expressing $Ca_v3.2$ (black, n = 12 cells) or $Ca_v3.2$ and CB_1 receptors (green, n = 13 cells). (c) Time course for perfusion of 3 μM CBD in cells expressing $Ca_v2.2$ and CB_1 receptors (green, n = 5 cells). (d) IV-curves of cells expressing $Ca_v3.2$ before (black) and after perfusion of 3 μM CBD (grey, n = 9 cells). (e) IV-curves of cells expressing $Ca_v3.2$ and CB_1 receptors before (green) and after perfusion of 3 μM CBD (light green, n = 8 cells). (f) Steady-state inactivation of cells expressing $Ca_v3.2$ before (black) and after perfusion of 3 μM CBD (grey, n = 9 cells). (g) Steady-state inactivation of cells expressing $Ca_v3.2$ before (green) and after perfusion of 3 μM CBD (light green, n = 9 cells). (h) Comparison of % inhibition of peak current density after perfusion of 3 μM CBD between cells expressing $Ca_v3.2$ only (grey, n = 9 cells) or $Ca_v3.2$ and CB_1 receptors (light green, n = 8 cells, Student's unpaired *t* test, $P > 0.05$). (i) Comparison of the magnitude of the shift in half inactivation voltage after perfusion of 3 μM CBD between cells expressing $Ca_v3.2$ only (grey, n = 9 cells) or $Ca_v3.2$ and CB_1 receptors (light green, n = 8 cells, Student's unpaired *t* test, $P > 0.05$). (j) Sample trace of inward current before (black) and after (green) perfusion of 3 μM CBD in acutely isolated DRG neurons. (k) Quantification of % inhibition by CBD of inward current in response to voltage steps to −30 mV in DRG neurons (n = 6 neurons).

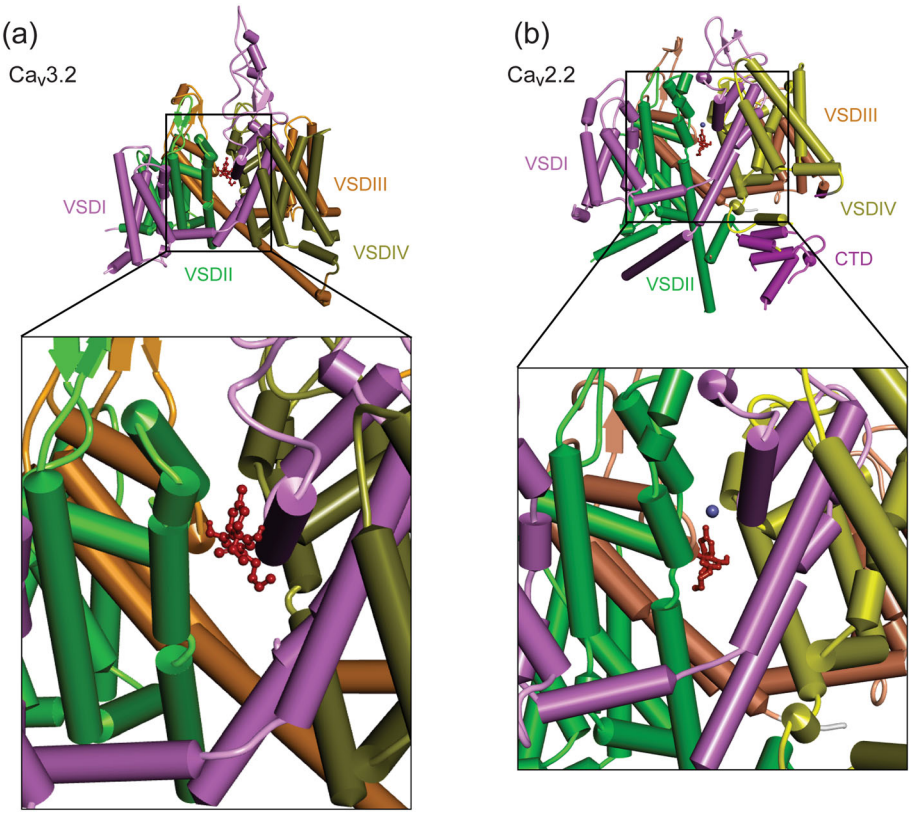

FIGURE 5 Molecular docking of cannabidiol (CBD) into $Ca_v3.2$ and $Ca_v2.2$ channels supports block of the $Ca_v3.2$ but not the $Ca_v2.2$ pore. (a) Top-sectional view of a homology model of $Ca_v3.2$ with CBD (red). (b) Top-sectional view of the cryo-EM structure of $Ca_v2.2$ with CBD (red). Voltage-sensing domains (VSDs) coloured in purple (I), green (II), orange (III), and yellow (IV), with the C-terminal domain in indigo.

$Ca_v3.2$, binding of CBD to $Ca_v2.2$ produces hydrogen bonds with Leu1352 and Leu1356, alkyl interactions with Leu1352, Leu1356 and Met1293; π-alkyl interactions with Phe1693, Phe1359, Val1689, Leu1356 and Trp1353 and an π-sigma interaction with Tyr1685 (Figure S2). Notably, CBD does not bind with DII-DIII domains, W-helix sites, or any other hydrophobic residues like W768, S764-A783, Y1289 and F1411 that are critical to the inhibition produced by other antagonists like **ziconotide (ω-conotoxin MVIIA)**, PD173212 and $Ca_v2.2$ blocker 1 (Dong et al., 2021; Gao et al., 2021). Thus, CBD may cause less pore occlusion and no stabilization of the inactivated $Ca_v2.2$ channel. Together, these data support our electrophysiological findings that CBD produces direct inhibition of $Ca_v3.2$, but not $Ca_v2.2$.

3.5 | Spinal administration of CBD produces analgesia through a $Ca_v3.2$-dependent mechanism

To further characterize the potential analgesic effects of CBD at the spinal level, intrathecal (i.t.) administration of CBD was performed in several mouse pain models (Figure 6a). First, formalin was injected into one hindpaw of male mice to induce acute inflammatory pain (Hunskaar et al., 1985). Next, either vehicle or different doses of CBD were administered i.t. to investigate the potential threshold for which an analgesic effect could be observed. Formalin produced nocifensive responses in both the first and second phases as observed in vehicle-treated mice (Figure 6b). While 3 μg CBD did not produce significant reductions in nocifensive responses, we found that 10 μg CBD significantly reduced the duration of nocifensive responses in both phases. We therefore tested 10 μg CBD in both inflammatory and neuropathic models of chronic pain.

Complete Freund's Adjuvant (CFA) was injected into one hindpaw of male mice as a model of inflammatory pain (Ferreira et al., 2001). Whereas control mice injected with PBS displayed stable thermal paw withdrawal latencies over a 180-min time course, mice injected with CFA that were given vehicle displayed significantly lower thermal latencies (Figure 6c). Conversely, mice injected with CFA that were given i.t. CBD (10 μg) showed a significant amelioration of thermal hypersensitivity at both 30 and 60 min after CBD injection.

Given that there are sex differences in both acute and chronic pain (Dedek et al., 2022; Rosen et al., 2017; Sorge et al., 2015), we next sought to determine if CBD can also produce analgesia in female mice. Using the same paradigm of CFA and i.t. CBD, we investigated a single time point 45 min after CBD administration for potential analgesic effects (Figure 6d). Female mice displayed significantly lowered thermal withdrawal latency when injected with CFA as compared to PBS. 45 min after CBD administration, CFA-injected mice treated with CBD had greater withdrawal latencies, which were no longer significantly different than mice treated with PBS instead of CFA. Together, these data indicate that i.t. CBD is effective in treating inflammatory pain in both male and female mice at doses as low as 10 μg.

In additional experiments, we investigated whether this dose of i.t. CBD also alleviates mechanical hypersensitivity induced by

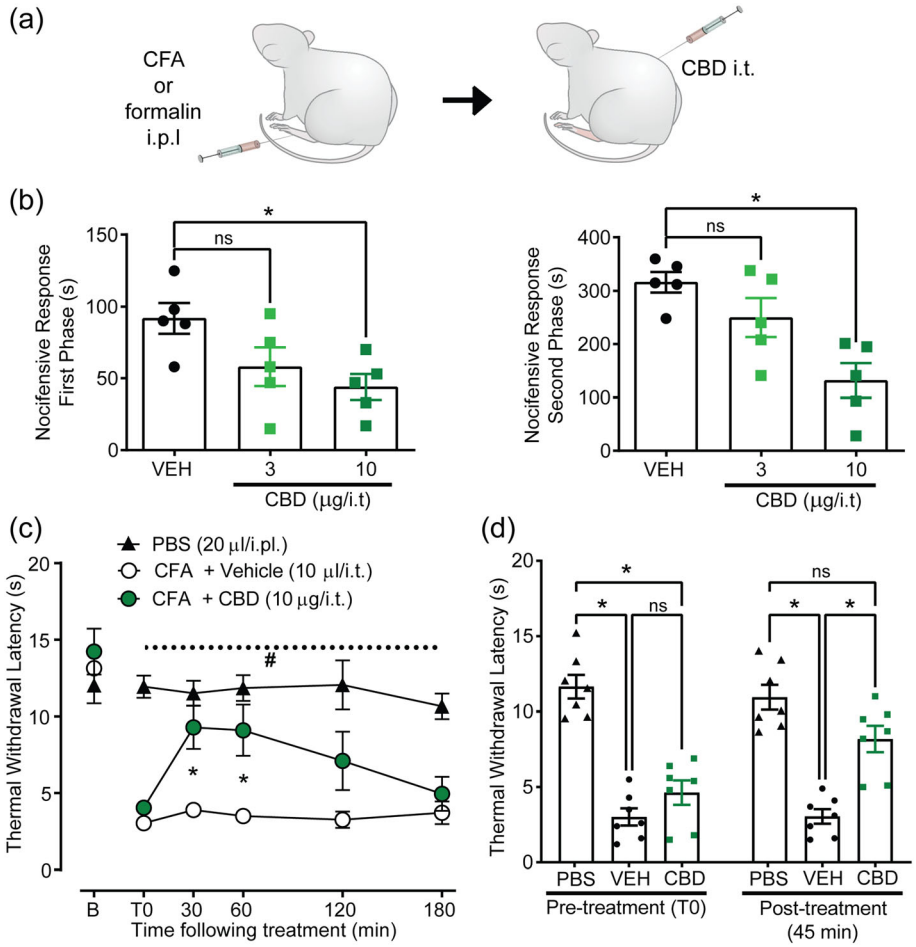

FIGURE 6 Spinal administration of cannabidiol (CBD) produces analgesia in formalin and CFA inflammatory pain models. (a) Schematic depicting the utilized behavioural paradigm. (b) Dose–response comparisons of the effect of CBD (3 and 10 µg, i.t.) versus vehicle (2.5% DMSO in PBS) on nocifensive response times during first and second phases of the formalin test. Analysed by one-way ANOVAs with post hoc Holm–Sidak comparisons ($P < 0.05$ for first phase, $P < 0.05$ for second phase, n = 5 male mice for all tests). (c) Time course of the effect of CBD (green, 10 µg, i.t., n = 7 male mice) versus vehicle (white, n = 6 male mice) on thermal hypersensitivity induced by Complete Freund's Adjuvant (CFA) injection, revealing a maximal effect between 30–60 min after i.t. injection. Analysed by two-way ANOVA, CBD treatment $P < 0.05$, time $P > 0.05$. PBS-treated mice shown in black (n = 6 male mice), with comparison to CFA-treated mice, as analysed by two-way ANOVA, CFA treatment $P < 0.05$, time $P > 0.05$. Holm–Sidak post hoc comparisons between vehicle and CBD-treated mice shown as *, for PBS- and CBD-treated mice as #. (d) Effect of CBD (green, 10 µg, i.t., n = 7 female mice) on CFA-treated female mice as compared to vehicle (black circles, n = 7 female mice) or PBS-treated mice (black triangles, n = 7 mice). Analysed by two-way ANOVA, condition $P > 0.05$, before versus after treatment $P < 0.05$, interaction $P < 0.05$, followed by Holm–Sidak post hoc comparisons.

neuropathic pain. In male mice with the partial sciatic nerve ligation (PSNL) model of neuropathic pain, we found that mechanical withdrawal threshold was significantly lower than that of sham operated mice (Figure 7a,b). Mice treated with CBD displayed a greater mechanical withdrawal threshold as compared to vehicle-treated mice, which was not significantly different than sham mice. Therefore, i.t. CBD also produces significant analgesia in neuropathic models of chronic pain.

Finally, we investigated whether the antinociceptive effect of spinal CBD administration was through $Ca_v3.2$ inhibition. $Ca_v3.2$ null mice have compensatory mechanisms that allow them to develop chronic inflammatory pain in the CFA model (Bourinet et al., 2005; García-Caballero et al., 2014), thus making these mice a convenient model to probe the role of Cav3.2 channels in the analgesic effects of CBD. Male wild-type and $Ca_v3.2$ null mice were injected with CFA into one hindpaw (Figure 7c). Baseline measurements of thermal withdrawal latency were consistent with thermal hypersensitivity in both wild-type and $Ca_v3.2$ null mice. Mice were then injected with a saturating dose of i.t. CBD (100 µg) to produce maximal analgesia and thermal withdrawal latencies were measured again 45 min after administration. We found that while wild-type mice displayed thermal thresholds consistent with reversal of thermal hypersensitivity, $Ca_v3.2$ null mice treated with CBD showed no significant analgesic effect. Therefore, when spinally administered, CBD produces analgesia that relies predominantly on the presence of $Ca_v3.2$ channels.

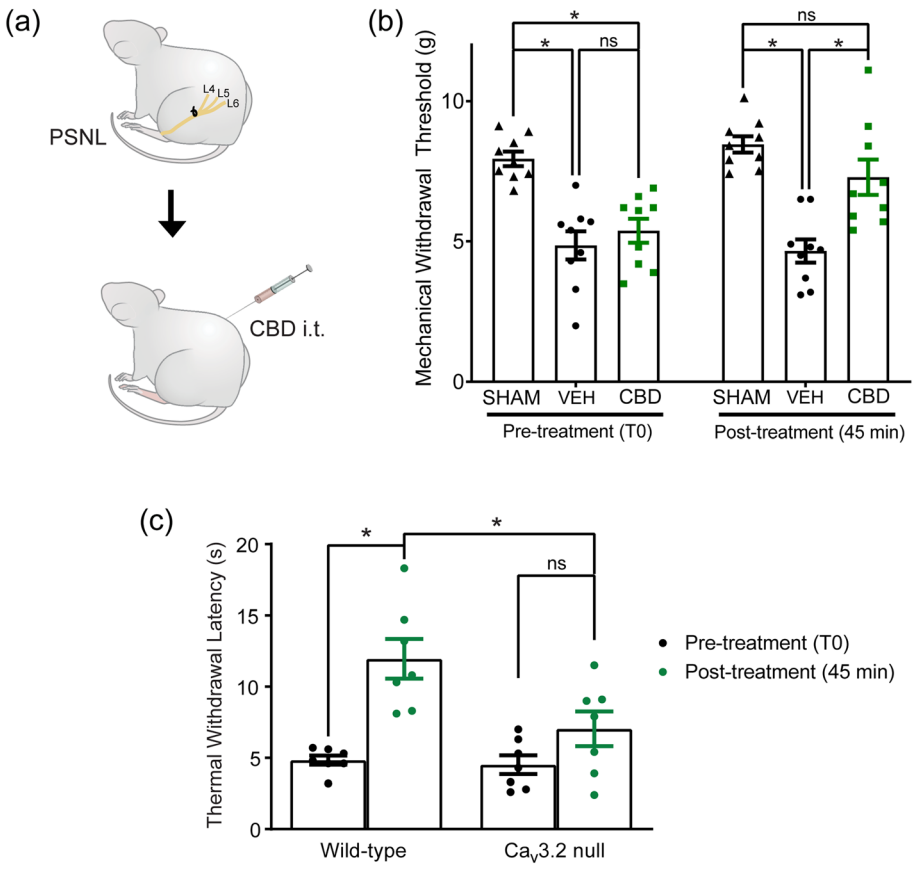

FIGURE 7 Spinal administration of cannabidiol (CBD) produces analgesia through a $Ca_v3.2$-dependent mechanism. (a) Schematic depicting the utilized behavioural paradigm of partial sciatic nerve ligation (PSNL) and intrathecal (i.t.) CBD administration. (b) Effect of CBD (green, 10 μg, i.t., n = 9 mice) on mechanical withdrawal threshold in male mice with PSNL as compared to vehicle (black circles, n = 9 mice) or sham surgery mice (black triangles, n = 9 mice). Analysed by two-way ANOVA, condition $P < 0.05$, before versus after treatment $P < 0.05$, followed by Holm–Sidak post hoc comparisons. (c) Effect of CBD (100 μg, i.t.) on CFA-induced thermal hypersensitivity as measured via a Hargreave's apparatus in male wild-type (n = 7 mice) and $Ca_v3.2$ null mice (n = 7 mice). Analysed by two-way ANOVA, CBD treatment $P < 0.05$, wild-type versus $Ca_v3.2$ null $P < 0.05$, interaction $P < 0.05$, followed by Holm–Sidak post hoc comparisons.

4 | DISCUSSION

In this study, we investigated the action of CB_1 receptors on representative members of the Ca_v2 and Ca_v3 calcium channel families that are known to be involved in afferent pain signalling. G protein-mediated inhibition of $Ca_v2.2$ by CB_1 receptor activation has been well documented (de Waard et al., 2005; Demuth & Molleman, 2006; Mackie & Hille, 1992; Twitchell et al., 1997). Many types of GPCRs mediate voltage-dependent modulation of $Ca_v2.2$ channels by direct interaction of Gβγ to the N-terminus region and domain I-II linker region of the pore forming Ca_v2 α1 subunit (Agler et al., 2005; de Waard et al., 2005). This produces inhibition that is effectively reversed with a strong depolarizing prepulse and as we show here, this is also true for CB_1 receptors. In contrast, members of the Ca_v3 calcium channel family do not typically undergo this type of membrane delimited voltage-dependent modulation and our data are consistent with this notion. The only direct G protein modulation of $Ca_v3.2$ calcium channels has been reported specifically for Gβ2γ2 dimers (DePuy et al., 2006; Wolfe et al., 2003), with an effect on open probability but a lack of voltage dependence. We did not observe CB_1 receptor-mediated modulation of $Ca_v3.2$, suggesting that this receptor does not couple effectively to Gβ2γ2. We note that G protein-coupled receptors modulate $Ca_v3.2$ channel activity via other types of signalling pathways. This includes signalling via the **corticotropin-releasing factor receptor 1 (CEF_1 receptor)** (Tao et al., 2008), **dopamine D_1 receptors** (Hu et al., 2009) and **neurokinin NK_1 receptor**) (Rangel et al., 2010). However, these GPCRs are coupled to stimulatory Gα proteins, whereas CB_1 receptor is coupled to inhibitory Gαi/o proteins, which could explain why no modulation was observed in our experiments.

We also observed that CB_1 receptors co-immunoprecipitated with both calcium channel isoforms. The existence of such signalling complexes with $Ca_v2.2$ can serve to optimize receptor-mediated modulation of the channel channels and may allow for receptor-mediated channel trafficking to and from the cell surface. This has been reported for several types of GPCRs that associate with $Ca_v2.2$, such as **nociceptin opioid peptide receptor (NOP/ORL1)** and D_1 and **D_2 receptors** (Altier et al., 2006; Beedle & Zamponi, 2004; Kisilevsky et al., 2008; Kisilevsky & Zamponi, 2008). Given that $Ca_v2.2$ channels can be co-internalized with various types of GPCRs, and that the CB_1 receptor internalizes upon prolonged agonist stimulation (Hsieh et al., 1999; Jin et al., 1999), it will be interesting to explore in further studies whether the CB_1 receptor can regulate $Ca_v2.2$ channel trafficking. We could not find any evidence that co-expression of CB_1 receptors changes $Ca_v3.2$ expression or function either basally, or in the presence of HU-210. The significance of the association between CB_1 receptors and $Ca_v3.2$ needs to be explored further, but this binding interaction could be responsible for specific subcellular targeting of this complex in neurons.

Consistent with previous studies (Pertwee, 2008), we found that micromolar concentrations of CBD did not produce sufficient activation of CB_1 receptors to inhibit $Ca_v2.2$, nor did we observe direct inhibition of this channel. Instead, we found that CBD directly inhibited $Ca_v3.2$ in a CB_1 receptor-independent manner. These findings are consistent with those reported by Ross and colleagues, who also found a CBD induced hyperpolarizing shift in the half-inactivation potential of $Ca_v3.2$ (Ross et al., 2008). Within our experimental conditions, we observed an IC50 of 4.06 μM, which is slightly lower than that reported by Ross et al. However, this could be explained by differences in external and internal recording solutions, differences in charge carrier, or by differences in cell lines that were used. Importantly, we found that higher concentrations of CBD (>10 μM) produced near complete inhibition of $Ca_v3.2$. Together, these results indicate that CBD has a moderate affinity towards $Ca_v3.2$, but that its interaction can fully occlude channel function at sufficiently high concentrations. Dose dependence becomes especially important in considering potential clinical implications. In clinical studies utilizing CBD, doses up to 50 $mg \cdot kg^{-1}$ daily may be administered (Millar et al., 2019; Sholler et al., 2020), which suggests that inhibition of $Ca_v3.2$ by CBD could be a viable mechanism through which analgesia is achieved. While CBD is considered to generally have a good safety profile, it should be noted that doses exceeding 200 $mg \cdot kg^{-1}$ have shown side effects in preclinical animal models, including effects on foetal development and spermatogenesis (Huestis et al., 2019; Iffland & Grotenhermen, 2017).

Despite the differential effect of CBD on $Ca_v2.2$ and $Ca_v3.2$, our molecular modelling indicates that both channel isoforms can interact with CBD, at least *in silico*, with high binding energy. The molecular docking was performed using a homology model of $Ca_v3.2$ that we created *de novo*. We note that a recent report by Rangel-Galvan and colleagues also showed a $Ca_v3.2$ homology model that was used for docking of cannabinoid-derived small organic blockers of $Ca_v3.2$ (Rangel-Galván et al., 2022) and displayed similar structural arrangement of the voltage-sensing domain but did show some differences in the pore domains. However, consistent with our findings with CBD, the synthetic cannabinoid derivatives examined by these authors docked most effectively within the pore region of $Ca_v3.2$. The interactions with the S6 segment are consistent with a stabilization of the inactivated state as observed in our electrophysiological analysis. Our molecular docking analysis also reveals that CBD can dock near the pore of $Ca_v2.2$ but does so without fully occluding the permeation pathway, thus explaining why $Ca_v2.2$ channels are not blocked by this compound. Furthermore, this type of analysis may offer useful in silico approaches towards identification of new chemical compounds that can block the $Ca_v3.2$ channel.

Several other cannabinoids and terpenes can also directly inhibit $Ca_v3.2$, including **anandamide** (Chemin et al., 2001), THC (Ross et al., 2008), a myriad of phytocannabinoids found in cannabis (Mirlohi et al., 2022), endogenous lipoamines (Barbara et al., 2009) and terpenes such as α-bisabolol and camphene (Gadotti et al., 2021). Additionally, studies have found that synthetic cannabinoids are capable of inhibiting $Ca_v3.2$ (Kevin et al., 2022), including HU-210 at higher concentrations (Chemin et al., 2001) However, in our experimental paradigm, concentrations up to 5 μM HU-210 did not affect $Ca_v3.2$ current, allowing us to assess CB_1 receptor activation independently of direct $Ca_v3.2$ inhibition.

The wide variety of cannabinoids that can inhibit $Ca_v3.2$ and other Ca_v3 channels suggests a conserved mechanism for binding that could be utilized for development of novel inhibitors for these channels. Indeed, using cannabinoid receptor agonists as lead compounds for development of new mixed CB_1 receptor agonists/Ca_v3 inhibitors has produced several promising compounds (Berger et al., 2014; Bladen et al., 2015; Gadotti et al., 2013; Kevin et al., 2022; You et al., 2011). Of particular interest is that many of these compounds can produce analgesia *in vivo*, representing potential novel therapeutics.

We found evidence that when administered intrathecally, the analgesic effect of CBD is prevented in $Ca_v3.2$ null mice. This provides the first evidence that CBD may produce analgesia through inhibition of $Ca_v3.2$ present at either nociceptive presynaptic terminals or in spinal interneurons within the dorsal horn (Candelas et al., 2019; François et al., 2015; Harding et al., 2021). The targeting of $Ca_v3.2$ as a potential pain treatment has a great deal of preclinical evidence in rodent models, and preliminary phase 1 and 1b trials in humans suggest that it is a viable target (Lee, 2014). We note that this experiment was specifically designed to assess the activity of CBD at the spinal level, with intrathecal delivery bypassing metabolic stages and blood brain barrier permeation. Thus, when administered orally or through inhalation, it is possible that the analgesic effects of CBD could be altered due to metabolism of CBD (Huestis, 2005; Lucas et al, 2018). Additionally, given that CBD can modulate several other channels, it is likely that there are multiple other supraspinal or peripheral mechanisms through which CBD could produce analgesia. Supporting this, several potential mechanisms for analgesia derived by CBD administration have been demonstrated. For example, in a model of osteoarthritis, peripherally administered CBD produced analgesia, which was occluded by systemic **CB_2** or TRPV1 receptor antagonists (Philpott et al., 2017). Several studies now also implicate analgesia and anxiolytic effects by CBD administration through action at $5\text{-}HT_{1A}$ receptors within the brain (de Gregorio et al., 2019; King et al., 2017; Ward et al., 2014).

In our experiments, intrathecal doses as low as 10 μg CBD were sufficient to produce analgesic effects in mouse models of both inflammatory and neuropathic pain. In examining the time course of analgesic efficacy, we found that CBD increased thermal withdrawal latency at both 30 and 60 min after injection such that CFA-treated mice no longer had statistically significant differences in withdrawal latency as compared to PBS-injected mice. Importantly, we found that CBD-induced analgesia was observed in both male and female mice, suggesting that the mechanism underlying analgesia was not sexually divergent. While several other potential analgesic targets show differential effects in males and females (Dedek et al., 2022; Sorge et al., 2015), inhibition of Ca_v3 channels by the selective antagonist

Z944 produces analgesia in both male and female rodents with inflammatory pain (Harding et al., 2021) Together, our results further implicate targeting of spinal $Ca_v3.2$ channels as a viable target for treatment of chronic pain.

5 | CONCLUSION

Our data demonstrate that cannabinoid-mediated inhibition of high voltage-activated calcium channels like $Ca_v2.2$ occurs through CB_1 receptor-dependent mechanisms, whereas low voltage-activated calcium channels like $Ca_v3.2$ can only be inhibited directly by certain cannabinoids such as CBD. Furthermore, the lack of analgesic effect in $Ca_v3.2$ null mice implicates $Ca_v3.2$ as a potential target for CBD-mediated analgesia at the spinal level.

AUTHOR CONTRIBUTIONS

Erika K. Harding, Gerald W. Zamponi and Tuan Trang conceptualized the study and wrote the manuscript. Erika K. Harding, Ivana A. Souza, Maria A. Gandini and Sun Huang performed electrophysiological recordings. Ivana A. Souza and Maria A. Gandini performed co-immunoprecipitation assays. Vinícius M. Gadotti and Flavia T.T. Antunes performed behavioural experiments. Md Yousof Ali performed homology modelling and docking simulations. Erika K. Harding, Ivana A. Souza, Maria A. Gandini, Sun Huang and Vinícius M. Gadotti performed data analysis. All authors contributed to reviewing and editing of the manuscript.

ACKNOWLEDGEMENTS

We thank Lina Chen for technical support in maintenance and transfection of tsA-201 cultures. We also thank Dr. Ken Mackie for providing the CB_1 receptor plasmid and Dr. Terrance Snutch for providing the $Ca_v3.2$ and $Ca_v2.2$ receptor plasmids. We thank Dr. Churmy Fan for providing support with illustrations of behavioural experiments. This work was supported by grants from Alberta Innovates mCannabis program and the Canadian Institutes of Health Research (CIHR) awarded to T.T. and G.W.Z. G.W.Z holds a Canada Research Chair. E.K.H and F.T.T.A. were supported by an Eyes High Fellowship and E.K.H by a SCNIP fellowship. M.Y.A. is supported by a Mitacs postdoctoral fellowship with Zymedyne Therapeutics.

CONFLICT OF INTEREST

None of the authors have a conflict of interest arising from this work.

DECLARATION OF TRANSPARENCY AND SCIENTIFIC RIGOUR

This Declaration acknowledges that this paper adheres to the principles for transparent reporting and scientific rigour of preclinical research as stated in the *BJP* guidelines for Design and Analysis, Immunoblotting and Immunochemistry and Animal Experimentation, and as recommended by funding agencies, publishers and other organizations engaged with supporting research.

DATA AVAILABILITY STATEMENT

The data that support the findings of this study are available from the corresponding author upon reasonable request. Some data may not be made available because of privacy or ethical restrictions.

ORCID

Gerald W. Zamponi https://orcid.org/0000-0002-0644-9066

REFERENCES

Agler, H. L., Evans, J., Tay, L. H., Anderson, M. J., Colecraft, H. M., & Yue, D. T. (2005). G protein-gated inhibitory module of N-type ($Ca_V2.2$) Ca^{2+} channels. *Neuron*, *46*(6), 891–904. https://doi.org/10.1016/j.neuron.2005.05.011

Alexander, S. P., Christopoulos, A., Davenport, A. P., Kelly, E., Mathie, A., Peters, J. A., Veale, E. L., Armstrong, J. F., Faccenda, E., Harding, S. D., Pawson, A. J., Southan, C., Davies, J. A., Abbracchio, M. P., Alexander, W., Al-hosaini, K., Bäck, M., Barnes, N. M., Bathgate, R., … Ye, R. D. (2021). THE CONCISE GUIDE TO PHARMACOLOGY 2021/22: G protein-coupled receptors. *British Journal of Pharmacology*, *178*(S1), S27–S156. https://doi.org/10.1111/bph.15538

Alexander, S. P., Mathie, A., Peters, J. A., Veale, E. L., Striessnig, J., Kelly, E., Armstrong, J. F., Faccenda, E., Harding, S. D., Pawson, A. J., Southan, C., Davies, J. A., Aldrich, R. W., Attali, B., Baggetta, A. M., Becirovic, E., Biel, M., Bill, R. M., Catterall, W. A., … Zhu, M. (2021). THE CONCISE GUIDE TO PHARMACOLOGY 2021/22: Ion channels. *British Journal of Pharmacology*, *178*(S1), S157–S245. https://doi.org/10.1111/bph.15539

Alexander, S. P. H., Roberts, R. E., Broughton, B. R. S., Sobey, C. G., George, C. H., Stanford, S. C., Cirino, G., Docherty, J. R., Giembycz, M. A., Hoyer, D., Insel, P. A., Izzo, A. A., Ji, Y., MacEwan, D. J., Mangum, J., Wonnacott, S., & Ahluwalia, A. (2018). Goals and practicalities of immunoblotting and immunohistochemistry: A guide for submission to the British Journal of Pharmacology. *British Journal of Pharmacology*, *175*(3), 407–411. https://doi.org/10.1111/bph.14112

Altier, C., Khosravani, H., Evans, R. M., Hameed, S., Peloquin, J. B., Vartian, B. A., Chen, L., Beedle, A. M., Ferguson, S. S. G., Mezghrani, A., Dubel, S. J., Bourinet, E., McRory, J. E., & Zamponi, G. W. (2006). ORL1 receptor-mediated internalization of N-type calcium channels. *Nature Neuroscience*, *9*, 31–40. https://doi.org/10.1038/nn1605

Altier, C., & Zamponi, G. W. (2008). Signaling complexes of voltage-gated calcium channels and G protein-coupled receptors. *Journal of Receptors and Signal Transduction*, *28*, 71–81. https://doi.org/10.1080/10799890801941947

Barbara, G., Alloui, A., Nargeot, J., Lory, P., Eschalier, A., Bourinet, E., & Chemin, J. (2009). T-type calcium channel inhibition underlies the analgesic effects of the endogenous lipoamino acids. *Journal of Neuroscience*, *29*(42), 13106–13114. https://doi.org/10.1523/JNEUROSCI.2919-09.2009

Baron, E. P., Lucas, P., Eades, J., & Hogue, O. (2018). Patterns of medicinal cannabis use, strain analysis, and substitution effect among patients with migraine, headache, arthritis, and chronic pain in a medicinal cannabis cohort. *Journal of Headache and Pain*, *19*(1), 37. https://doi.org/10.1186/s10194-018-0862-2

Beedle, A. M., & Zamponi, G. W. (2004). Modulation of high voltage-activated calcium channels by G protein-coupled receptors. In *Calcium Channel Pharmacology* (pp. 331–367). Springer. https://doi.org/10.1007/978-1-4419-9254-3_10

Berger, N. D., Gadotti, V. M., Petrov, R. R., Chapman, K., Diaz, P., & Zamponi, G. W. (2014). NMP-7 inhibits chronic inflammatory and neuropathic pain via block of Cav3.2T-type calcium channels and activation of CB2 receptors. *Molecular Pain*, *10*, 77. https://doi.org/10.1186/1744-8069-10-77

Bisogno, T., Hanuš, L., de Petrocellis, L., Tchilibon, S., Ponde, D. E., Brandi, I., Moriello, A. S., Davis, J. B., Mechoulam, R., & di Marzo, V. (2001). Molecular targets for cannabidiol and its synthetic analogues: Effect on vanilloid VR1 receptors and on the cellular uptake and enzymatic hydrolysis of anandamide. *British Journal of Pharmacology*, *134*(4), 845–852. https://doi.org/10.1038/sj.bjp.0704327

Bladen, C., McDaniel, S. W., Gadotti, V. M., Petrov, R. R., Berger, N. D., Diaz, P., & Zamponi, G. W. (2015). Characterization of novel cannabinoid based T-type calcium channel blockers with analgesic effects. *ACS Chemical Neuroscience*, *6*(2), 277–287. https://doi.org/10.1021/cn500206a

Boehnke, K. F., Litinas, E., & Clauw, D. J. (2016). Medical cannabis use is associated with decreased opiate medication use in a retrospective cross-sectional survey of patients with chronic pain. *The Journal of Pain*, *17*(6), 739–744. https://doi.org/10.1016/j.jpain.2016.03.002

Bourinet, E., Alloui, A., Monteil, A., Barrère, C., Couette, B., Poirot, O., Pages, A., McRory, J., Snutch, T. P., Eschalier, A., & Nargeot, J. (2005). Silencing of the $Ca_v3.2$ T-type calcium channel gene in sensory neurons demonstrates its major role in nociception. *The EMBO Journal*, *24*(2), 315–324. https://doi.org/10.1038/sj.emboj.7600515

Candelas, M., Reynders, A., Arango-Lievano, M., Neumayer, C., Fruquière, A., Demes, E., Hamid, J., Lemmers, C., Bernat, C., Monteil, A., Compan, V., Laffray, S., Inquimbert, P., le Feuvre, Y., Zamponi, G. W., Moqrich, A., Bourinet, E., & Méry, P. F. (2019). Cav3.2 T-type calcium channels shape electrical firing in mouse Lamina II neurons. *Scientific Reports*, *9*, 3112. https://doi.org/10.1038/s41598-019-39703-3

Chemin, J., Monteil, A., Perez-Reyes, E., Nargeot, J., & Lory, P. (2001). Direct inhibition of T-type calcium channels by the endogenous cannabinoid anandamide. *EMBO Journal*, *20*(24), 7033–7040. https://doi.org/10.1093/emboj/20.24.7033

Chen, C. C., Lamping, K. G., Nuno, D. W., Barresi, R., Prouty, S. J., Lavoie, J. L., Cribbs, L. L., England, S. K., Sigmund, C. D., Weiss, R. M., Williamson, R. A., Hill, J. A., & Campbell, K. P. (2003). Abnormal coronary function in mice deficient in α_{1H} T-type Ca^{2+} channels. *Science*, *302*(5649), 1416–1418. https://doi.org/10.1126/science.1089268

Curtis, M. J., Alexander, S. P. H., Cirino, G., George, C. H., Kendall, D. A., Insel, P. A., Izzo, A. A., Ji, Y., Panettieri, R. A., Patel, H. H., Sobey, C. G., Stanford, S. C., Stanley, P., Stefanska, B., Stephens, G. J., Teixeira, M. M., Vergnolle, N., & Ahluwalia, A. (2022). Planning experiments: Updated guidance on experimental design and analysis and their reporting III. *British Journal of Pharmacology*, *179*(15), 3907–3913. https://doi.org/10.1111/bph.15868

de Gregorio, D., McLaughlin, R. J., Posa, L., Ochoa-Sanchez, R., Enns, J., Lopez-Canul, M., Aboud, M., Maione, S., Comai, S., & Gobbi, G. (2019). Cannabidiol modulates serotonergic transmission and reverses both allodynia and anxiety-like behavior in a model of neuropathic pain. *Pain*, *160*(1), 136–150. https://doi.org/10.1097/j.pain.0000000000001386

de Waard, M., Hering, J., Weiss, N., & Feltz, A. (2005). How do G proteins directly control neuronal Ca^{2+} channel function? *Trends in Pharmacological Sciences*, *26*(8), 427–436. https://doi.org/10.1016/j.tips.2005.06.008

Dedek, A., Xu, J., Lorenzo, L. É., Godin, A. G., Kandegedara, C. M., Glavina, G., Landrigan, J. A., Lombroso, P. J., de Koninck, Y., Tsai, E. C., & Hildebrand, M. E. (2022). Sexual dimorphism in a neuronal mechanism of spinal hyperexcitability across rodent and human models of pathological pain. *Brain*, *145*(3), 1124–1138. https://doi.org/10.1093/brain/awab408

Demuth, D. G., & Molleman, A. (2006). Cannabinoid signalling. *Life Sciences*, *78*(6), 549–563. https://doi.org/10.1016/j.lfs.2005.05.055

DePuy, S. D., Yao, J., Hu, C., McIntire, W., Bidaud, I., Lory, P., Rastinejad, F., Gonzalez, C., Garrison, J. C., & Barrett, P. Q. (2006). The molecular basis for T-type Ca^{2+} channel inhibition by G protein $\beta2\gamma2$ subunits. *Proceedings of the National Academy of Sciences of the United States of America*, *103*(39), 14590–14595. https://doi.org/10.1073/pnas.0603945103

di Marzo, V., Bifulco, M., & de Petrocellis, L. (2004). The endocannabinoid system and its therapeutic exploitation. *Nature Reviews Drug Discovery*, *3*(9), 771–784. https://doi.org/10.1038/nrd1495

Dong, Y., Gao, Y., Xu, S., Wang, Y., Yu, Z., Li, Y., Li, B., Yuan, T., Yang, B., Zhang, X. C., Jiang, D., Huang, Z., & Zhao, Y. (2021). Closed-state inactivation and pore-blocker modulation mechanisms of human $Ca_v2.2$. *Cell Reports*, *37*(5), 109931. https://doi.org/10.1016/j.celrep.2021.109931

Ferreira, J., Campos, M. M., Pesquero, J. B., Araújo, R. C., Bader, M., & Calixto, J. B. (2001). Evidence for the participation of kinins in Freund's adjuvant-induced inflammatory and nociceptive responses in kinin B1 and B2 receptor knockout mice. *Neuropharmacology*, *41*(8), 1006–1012. https://doi.org/10.1016/S0028-3908(01)00142-3

Finn, D. P., Haroutounian, S., Hohmann, A. G., Krane, E., Soliman, N., & Rice, A. S. C. (2021). Cannabinoids, the endocannabinoid system, and pain: A review of preclinical studies. *Pain*, *162*, S5–S25. https://doi.org/10.1097/j.pain.0000000000002268

Fisher, E., Moore, R. A., Fogarty, A. E., Finn, D. P., Finnerup, N. B., Gilron, I., Haroutounian, S., Krane, E., Rice, A. S. C., Rowbotham, M., Wallace, M., & Eccleston, C. (2021). Cannabinoids, cannabis, and cannabis-based medicine for pain management: A systematic review of randomised controlled trials. *Pain*, *162*, S45–S66. https://doi.org/10.1097/j.pain.0000000000001929

François, A., Schüetter, N., Laffray, S., Sanguesa, J., Pizzoccaro, A., Dubel, S., Mantilleri, A., Nargeot, J., Noël, J., Wood, J. N., Moqrich, A., Pongs, O., & Bourinet, E. (2015). The low-threshold calcium channel Cav3.2 determines low-threshold mechanoreceptor function. *Cell Reports*, *10*(3), 370–382. https://doi.org/10.1016/j.celrep.2014.12.042

Gadotti, V. M., Caballero, A. G., Berger, N. D., Gladding, C. M., Chen, L., Pfeifer, T. A., & Zamponi, G. W. (2015). Small organic molecule disruptors of Cav3.2—USP5 interactions reverse inflammatory and neuropathic pain. *Molecular Pain*, *11*, 12. https://doi.org/10.1186/s12990-015-0011-8

Gadotti, V. M., Huang, S., & Zamponi, G. W. (2021). The terpenes camphene and alpha-bisabolol inhibit inflammatory and neuropathic pain via Cav3.2 T-type calcium channels. *Molecular Brain*, *14*, 1. https://doi.org/10.1186/s13041-021-00876-6

Gadotti, V. M., You, H., Petrov, R. R., Berger, N. D., Diaz, P., & Zamponi, G. W. (2013). Analgesic effect of a mixed T-type channel inhibitor/CB2 receptor agonist. *Molecular Pain*, *9*, 32. https://doi.org/10.1186/1744-8069-9-32

Gandini, M. A., Souza, I. A., Raval, D., Xu, J., Pan, Y. X., & Zamponi, G. W. (2019). Differential regulation of Cav2.2 channel exon 37 variants by alternatively spliced μ-opioid receptors. *Molecular Brain*, *12*, 98. https://doi.org/10.1186/s13041-019-0524-6

Gao, S., Yao, X., & Yan, N. (2021). Structure of human $Ca_v2.2$ channel blocked by the painkiller ziconotide. *Nature*, *596*(7870), 143–147. https://doi.org/10.1038/s41586-021-03699-6

García-Caballero, A., Gadotti, V. M., Stemkowski, P., Weiss, N., Souza, I. A., Hodgkinson, V., Bladen, C., Chen, L., Hamid, J., Pizzoccaro, A., Deage, M., François, A., Bourinet, E., & Zamponi, G. W. (2014). The deubiquitinating enzyme USP5 modulates neuropathic and inflammatory pain by enhancing $Ca_v3.2$ channel activity. *Neuron*, *83*(5), 1144–1158. https://doi.org/10.1016/j.neuron.2014.07.036

Goodsell, D. S., Morris, G. M., & Olson, A. J. (1996). Automated docking of flexible ligands: Applications of AutoDock. *Journal of Molecular Recognition*, *9*(1), 1–5. https://doi.org/10.1002/(SICI)1099-1352(199601)9:1<1::AID-JMR241>3.0.CO;2-6

Harding, E. K., Dedek, A., Bonin, R. P., Salter, M. W., Snutch, T. P., & Hildebrand, M. E. (2021). The T-type calcium channel antagonist, Z944, reduces spinal excitability and pain hypersensitivity. *British*

Journal of Pharmacology, *178*(17), 3517–3532. https://doi.org/10.1111/bph.15498

Harding, E. K., & Zamponi, G. W. (2022). Central and peripheral contributions of T-type calcium channels in pain. *Molecular Brain*, *15*(1), 39. https://doi.org/10.1186/s13041-022-00923-w

He, L., Yu, Z., Geng, Z., Huang, Z., Zhang, C., Dong, Y., Gao, Y., Wang, Y., Chen, Q., Sun, L., Ma, X., Huang, B., Wang, X., & Zhao, Y. (2022). Structure, gating, and pharmacology of human $Ca_V3.3$ channel. *Nature Communications*, *13*(1), 2084. https://doi.org/10.1038/s41467-022-29728-0

Hsieh, C., Brown, S., Derleth, C., & Mackie, K. (1999). Internalization and recycling of the CB1 cannabinoid receptor. *Journal of Neurochemistry*, *73*(2), 493–501. https://doi.org/10.1046/j.1471-4159.1999.0730493.x

Hu, C., DePuy, S. D., Yao, J., McIntire, W. E., & Barrett, P. Q. (2009). Protein kinase a activity controls the regulation of T-type $Ca_V3.2$ channels by Gβγ dimers. *Journal of Biological Chemistry*, *284*(12), 7465–7473. https://doi.org/10.1074/jbc.M808049200

Huestis, M. A. (2005). Pharmacokinetics and metabolism of the plant cannabinoids, Δ^9-tetrahydrocannabinol, cannabidiol and cannabinol. In *Handbook of experimental pharmacology*. Springer. https://doi.org/10.1007/3-540-26573-2_23

Huestis, M. A., Solimini, R., Pichini, S., Pacifici, R., Carlier, J., & Busardò, F. P. (2019). Cannabidiol adverse effects and toxicity. *Current Neuropharmacology*, *17*(10), 974–989. https://doi.org/10.2174/1570159x17666190603171901

Hunskaar, S., Fasmer, O. B., & Hole, K. (1985). Formalin test in mice, a useful technique for evaluating mild analgesics. *Journal of Neuroscience Methods*, *14*(1), 69–76. https://doi.org/10.1016/0165-0270(85)90116-5

Iffland, K., & Grotenhermen, F. (2017). An update on safety and side effects of cannabidiol: A review of clinical data and relevant animal studies. *Cannabis and Cannabinoid Research*, *2*(1), 139–154. https://doi.org/10.1089/can.2016.0034

Jesus, C. H. A., Ferreira, M. V., Gasparin, A. T., Rosa, E. S., Genaro, K., Crippa, J. A. S., Chichorro, J. G., & Cunha, J. M. (2022). Cannabidiol enhances the antinociceptive effects of morphine and attenuates opioid-induced tolerance in the chronic constriction injury model. *Behavioural Brain Research*, *435*, 114076. https://doi.org/10.1016/j.bbr.2022.114076

Jin, W., Brown, S., Roche, J. P., Hsieh, C., Celver, J. P., Kovoor, A., Chavkin, C., & Mackie, K. (1999). Distinct domains of the CB1 cannabinoid receptor mediate desensitization and internalization. *Journal of Neuroscience*, *19*(10), 3773–3780. https://doi.org/10.1523/jneurosci.19-10-03773.1999

Jones, G., Willett, P., Glen, R. C., Leach, A. R., & Taylor, R. (1997). Development and validation of a genetic algorithm for flexible docking. *Journal of Molecular Biology*, *267*(3), 727–748. https://doi.org/10.1006/jmbi.1996.0897

Kevin, R. C., Mirlohi, S., Manning, J. J., Boyd, R., Cairns, E. A., Ametovski, A., Lai, F., Luo, J. L., Jorgensen, W., Ellison, R., Gerona, R. R., Hibbs, D. E., McGregor, I. S., Glass, M., Connor, M., Bladen, C., Zamponi, G. W., & Banister, S. D. (2022). Putative synthetic cannabinoids MEPIRAPIM, 5F-BEPIRAPIM (NNL-2), and their analogues are T-type calcium channel (Ca_V3) inhibitors. *ACS Chemical Neuroscience*, *13*(9), 1395–1409. https://doi.org/10.1021/acschemneuro.1c00822

King, K. M., Myers, A. M., Soroka-Monzo, A. J., Tuma, R. F., Tallarida, R. J., Walker, E. A., & Ward, S. J. (2017). Single and combined effects of Δ^9-tetrahydrocannabinol and cannabidiol in a mouse model of chemotherapy-induced neuropathic pain. *British Journal of Pharmacology*, *174*(17), 2832–2841. https://doi.org/10.1111/bph.13887

Kisilevsky, A. E., Mulligan, S. J., Altier, C., Iftinca, M. C., Varela, D., Tai, C., Chen, L., Hameed, S., Hamid, J., MacVicar, B. A., & Zamponi, G. W. (2008). D1 receptors physically interact with N-type calcium channels to regulate channel distribution and dendritic calcium entry. *Neuron*, *58*, 557–570. https://doi.org/10.1016/j.neuron.2008.03.002

Kisilevsky, A. E., & Zamponi, G. W. (2008). D2 dopamine receptors interact directly with N-type calcium channels and regulate channel surface expression levels. *Channels*, *2*, 269–277. https://doi.org/10.4161/chan.2.4.6402

Laprairie, R. B., Bagher, A. M., Kelly, M. E. M., & Denovan-Wright, E. M. (2015). Cannabidiol is a negative allosteric modulator of the cannabinoid CB1 receptor. *British Journal of Pharmacology*, *172*(20), 4790–4805. https://doi.org/10.1111/bph.13250

Lee, M. (2014). Z944: A first in class T-type calcium channel modulator for the treatment of pain. *Journal of the Peripheral Nervous System*, *19*(S2), S11–S12. https://doi.org/10.1111/jns.12080_2

Lilley, E., Stanford, S. C., Kendall, D. E., Alexander, S. P. H., Cirino, G., Docherty, J. R., George, C. H., Insel, P. A., Izzo, A. A., Ji, Y., Panettieri, R. A., Sobey, C. G., Stefanska, B., Stephens, G., Teixeira, M., & Ahluwalia, A. (2020). ARRIVE 2.0 and the British Journal of Pharmacology: Updated guidance for 2020. *British Journal of Pharmacology*, *177*(16), 3611–3616. https://doi.org/10.1111/bph.15178

Lucas, C. J., Galettis, P., & Schneider, J. (2018). The pharmacokinetics and the pharmacodynamics of cannabinoids. *British Journal of Clinical Pharmacology*, *84*(11), 2477–2482. https://doi.org/10.1111/bcp.13710

Mackie, K., & Hille, B. (1992). Cannabinoids inhibit N-type calcium channels in neuroblastoma-glioma cells. *Proceedings of the National Academy of Sciences of the United States of America*, *89*(9), 3825–3829. https://doi.org/10.1073/pnas.89.9.3825

Malmberg, A. B., & Basbaum, A. I. (1998). Partial sciatic nerve injury in the mouse as a model of neuropathic pain: Behavioral and neuroanatomical correlates. *Pain*, *76*(1–2), 215–222. https://doi.org/10.1016/S0304-3959(98)00045-1

Millar, S. A., Stone, N. L., Bellman, Z. D., Yates, A. S., England, T. J., & O'Sullivan, S. E. (2019). A systematic review of cannabidiol dosing in clinical populations. *British Journal of Clinical Pharmacology*, *85*(9), 1888–1900. https://doi.org/10.1111/bcp.14038

Mirdita, M., Schütze, K., Moriwaki, Y., Heo, L., Ovchinnikov, S., & Steinegger, M. (2022). ColabFold: Making protein folding accessible to all. *Nature Methods*, *19*(6), 679–682. https://doi.org/10.1038/s41592-022-01488-1

Mirlohi, S., Bladen, C., Santiago, M. J., Arnold, J. C., McGregor, I., & Connor, M. (2022). Inhibition of human recombinant T-type calcium channels by phytocannabinoids in vitro. *British Journal of Pharmacology*, *179*, 4031–4043. https://doi.org/10.1111/bph.15842

Mlost, J., Bryk, M., & Starowicz, K. (2020). Cannabidiol for pain treatment: Focus on pharmacology and mechanism of action. *International Journal of Molecular Sciences*, *21*(22), 8870. https://doi.org/10.3390/ijms21228870

Percie du Sert, N., Hurst, V., Ahluwalia, A., Alam, S., Avey, M. T., Baker, M., Browne, W. J., Clark, A., Cuthill, I. C., Dirnagl, U., Emerson, M., Garner, P., Holgate, S. T., Howells, D. W., Karp, N. A., Lazic, S. E., Lidster, K., MacCallum, C. J., Macleod, M., … Würbel, H. (2020). The ARRIVE guidelines 2.0: Updated guidelines for reporting animal research. *British Journal of Pharmacology*, *177*(16), 3617–3624. https://doi.org/10.1111/bph.15193

Pertwee, R. G. (2008). Ligands that target cannabinoid receptors in the brain: From THC to anandamide and beyond. *Addiction Biology*, *13*(2), 147–159. https://doi.org/10.1111/j.1369-1600.2008.00108.x

Philpott, H. T., O'Brien, M., & McDougall, J. J. (2017). Attenuation of early phase inflammation by cannabidiol prevents pain and nerve damage in rat osteoarthritis. *Pain*, *158*(12), 2442–2451. https://doi.org/10.1097/j.pain.0000000000001052

Rangel, A., Sánchez-Armass, S., & Meza, U. (2010). Protein kinase C-mediated inhibition of recombinant T-type $Ca_V3.2$ channels by neurokinin 1 receptors. *Molecular Pharmacology*, *77*(2), 202–210. https://doi.org/10.1124/mol.109.058727

Rangel-Galván, M., Castro, M. E., Perez-Aguilar, J. M., Caballero, N. A., Rangel-Huerta, A., & Melendez, F. J. (2022). Theoretical study of the structural stability, chemical reactivity, and protein interaction for NMP compounds as modulators of the endocannabinoid system. *Molecules*, *27*(2), 414. https://doi.org/10.3390/molecules27020414

Rosen, S., Ham, B., & Mogil, J. S. (2017). Sex differences in neuroimmunity and pain. *Journal of Neuroscience Research*, *95*(1–2), 500–508. https://doi.org/10.1002/jnr.23831

Ross, H. R., Napier, I., & Connor, M. (2008). Inhibition of recombinant human T-type calcium channels by Δ^9-tetrahydrocannabinol and cannabidiol. *Journal of Biological Chemistry*, *283*(23), 16124–16134. https://doi.org/10.1074/jbc.M707104200

Sholler, D. J., Schoene, L., & Spindle, T. R. (2020). Therapeutic efficacy of cannabidiol (CBD): A review of the evidence from clinical trials and human laboratory studies. *Current Addiction Reports*, *7*(3), 405–412. https://doi.org/10.1007/s40429-020-00326-8

Sorge, R. E., Mapplebeck, J. C. S., Rosen, S., Beggs, S., Taves, S., Alexander, J. K., Martin, L. J., Austin, J.-S., Sotocinal, S. G., Chen, D., Yang, M., Shi, X. Q., Huang, H., Pillon, N. J., Bilan, P. J., Tu, Y., Klip, A., Ji, R.-R., Zhang, J., … Mogil, J. S. (2015). Different immune cells mediate mechanical pain hypersensitivity in male and female mice. *Nature Neuroscience*, *18*(8), 1081–1083. https://doi.org/10.1038/nn.4053

Tao, J., Hildebrand, M. E., Liao, P., Mui, C. L., Tan, G., Li, S., Snutch, T. P., & Tuck, W. S. (2008). Activation of corticotropin-releasing factor receptor 1 selectively inhibits $Ca_V3.2$ T-type calcium channels. *Molecular Pharmacology*, *73*(6), 1596–1609. https://doi.org/10.1124/mol.107.043612

Tedford, H. W., & Zamponi, G. W. (2006). Direct G protein modulation of Ca_V2 calcium channels. *Pharmacological Reviews*, *58*, 837–862. https://doi.org/10.1124/pr.58.4.11

Trott, O., & Olson, A. J. (2009). AutoDock Vina: Improving the speed and accuracy of docking with a new scoring function, efficient optimization, and multithreading. *Journal of Computational Chemistry*, *31*, 455–461. https://doi.org/10.1002/jcc.21334

Turner, R. W., Anderson, D., & Zamponi, G. W. (2011). Signaling complexes of voltage-gated calcium channels. *Channels*, *5*, 440–448. https://doi.org/10.4161/chan.5.5.16473

Twitchell, W., Brown, S., & Mackie, K. (1997). Cannabinoids inhibit N- and P/Q-type calcium channels in cultured rat hippocampal neurons. *Journal of Neurophysiology*, *78*(1), 43–50. https://doi.org/10.1152/jn.1997.78.1.43

Vela, J., Dreyer, L., Petersen, K. K., Arendt-Nielsen, L., Duch, K. S., & Kristensen, S. (2022). Cannabidiol treatment in hand osteoarthritis and psoriatic arthritis: A randomized, double-blind, placebo-controlled trial. *Pain*, *163*(6), 1206–1214. https://doi.org/10.1097/j.pain.0000000000002466

Ward, S. J., McAllister, S. D., Kawamura, R., Murase, R., Neelakantan, H., & Walker, E. A. (2014). Cannabidiol inhibits paclitaxel-induced neuropathic pain through 5-HT 1A receptors without diminishing nervous system function or chemotherapy efficacy. *British Journal of Pharmacology*, *171*(3), 636–645. https://doi.org/10.1111/bph.12439

Ware, M. A., Adams, H., & Guy, G. W. (2005). The medicinal use of cannabis in the UK: Results of a nationwide survey. *International Journal of Clinical Practice*, *59*(3), 291–295. https://doi.org/10.1111/j.1742-1241.2004.00271.x

Whiting, P. F., Wolff, R. F., Deshpande, S., di Nisio, M., Duffy, S., Hernandez, A. V., Keurentjes, J. C., Lang, S., Misso, K., Ryder, S., Schmidlkofer, S., Westwood, M., & Kleijnen, J. (2015). Cannabinoids for medical use: A systematic review and meta-analysis. *JAMA : The Journal of the American Medical Association*, *313*(24), 2456. https://doi.org/10.1001/jama.2015.6358

Wolfe, J. T., Wang, H., Howard, J., Garrison, J. C., & Barrett, P. Q. (2003). T-type calcium channel regulation by specific G-protein βγ subunits. *Nature*, *424*(6945), 209–213. https://doi.org/10.1038/nature01772

You, H., Gadotti, V. M., Petrov, R. R., Zamponi, G. W., & Diaz, P. (2011). Functional characterization and analgesic effects of mixed cannabinoid receptor/T-type channel ligands. *Molecular Pain*, *7*, 89. https://doi.org/10.1186/1744-8069-7-89

Zamponi, G. W. (2016). Targeting voltage-gated calcium channels in neurological and psychiatric diseases. *Nature Reviews. Drug Discovery*, *15*, 19–34. https://doi.org/10.1038/nrd.2015.5

Zhang, H. X. B., Heckman, L., Niday, Z., Jo, S., Fujita, A., Shim, J., Pandey, R., al Jandal, H., Jayakar, S., Barrett, L. B., Smith, J., Woolf, C. J., & Bean, B. P. (2022). Cannabidiol activates neuronal Kv7 channels. *eLife*, *11*, e73246. https://doi.org/10.7554/ELIFE.73246

Zhao, Y., Huang, G., Wu, Q., Wu, K., Li, R., Lei, J., Pan, X., & Yan, N. (2019). Cryo-EM structures of apo and antagonist-bound human $Ca_V3.1$. *Nature*, *576*(7787), 492–497. https://doi.org/10.1038/s41586-019-1801-3

SUPPORTING INFORMATION

Additional supporting information can be found online in the Supporting Information section at the end of this article.

How to cite this article: Harding, E. K., Souza, I. A., Gandini, M. A., Gadotti, V. M., Ali, M. Y., Huang, S., Antunes, F. T. T., Trang, T., & Zamponi, G. W. (2023). Differential regulation of $Ca_V3.2$ and $Ca_V2.2$ calcium channels by CB_1 receptors and cannabidiol. *British Journal of Pharmacology*, *180*(12), 1616–1633. https://doi.org/10.1111/bph.16035